Barometers behaving badly II: A critical evaluation of Cpx-only and Cpx-Liq thermobarometry in variably-hydrous arc magmas

Penny E. Wieser[1,2], Adam J.R. Kent[2], Christy B. Till[3]

1. **Corresponding author**: Penny_wieser@berkeley.edu. Department of Earth and Planetary Sciences, McCone Hall, UC Berkeley, 94720, USA
2. College of Earth, Ocean and Atmospheric Sciences, Oregon State University, 97331, USA
3. School of Earth and Space Exploration, Arizona State University, Tempe, AZ 85281, USA

Key Words

- Clinopyroxene
- Thermobarometry
- Subduction Zones
- Arc magmatism
- Magma Storage Conditions

ABSTRACT

The chemistry of erupted clinopyroxene crystals (±equilibrium liquids) have been widely used to deduce the pressures and temperatures of magma storage in volcanic arcs. However, the wide variety of different equations parametrizing the relationship between mineral and melt compositions and intensive variables such as pressure and temperature yield vastly different results, with implications for our interpretation of magma storage conditions. We use a new test dataset of N=505 Cpx-Liq pairs from variably-hydrous experiments at crustal conditions (0-13 kbar) to assess the performance of different thermobarometers, and identify the most accurate and precise expressions for application to subduction zone magmas. First, we assess different equilibrium tests, finding that comparing the measured and predicted EnFs and K_D (using Fe_t in both phases) are the most useful tests in arc magmas, while CaTs, CaTi and Jd tests have limited utility. We then apply further quality filters based on cation sums (3.95-4.05), number of analyses (N>5), and the presence of reported H_2O data in the liquid to obtain a filtered dataset (N=194). We use this filtered dataset to compare calculated versus experimental pressures and temperatures for different combinations of thermobarometers. A number of Cpx-Liq thermometers perform very well when liquid H_2O contents are known, although the Cpx composition contributes relatively little to the calculated temperature. Most Cpx-only thermometers perform very badly, greatly overestimating temperatures for hydrous experiments. Cpx-Liq and Cpx-only barometers show similar performance to one another, all showing low precision and systematic offsets (overestimating pressure for low P experiments, and underestimating pressure for High P expressions). We also assess the sensitivity of different equations to melt H_2O contents, which are poorly constrained in many natural systems. Overall, this work demonstrates that substantial work is needed to obtain precise and accurate estimates of magma storage depths from Cpx±Liq equilibrium in volcanic arcs. At present, Cpx-based barometry only provides

sufficient resolution to distinguish broad storage regions (e.g., upper, mid, lower crust), rather than ability to precisely and accurately locate magma reservoirs to compare to geophysical records.

1. INTRODUCTION

The composition of erupted clinopyroxene (Cpx) and Cpx-liquid (Liq) pairs are commonly used to calculate pressures (P) and temperatures (T) in a variety of igneous systems. Cpx is a stable phase over a very wide range of pressures, temperatures, melt compositions and oxygen fugacities (e.g., Costa, 2004; Nandedkar et al., 2014; Ulmer et al., 2018), meaning Cpx-based thermobarometry has broad utility and has been applied in a wide variety of tectonic settings. In this contribution we specifically focus on the use of Cpx-based thermobarometer to investigate storage conditions in magmas erupted in subduction zones (see Table. 1 for studies performing such calculations; Auer et al., 2013; Belousov et al., 2021; Cassidy et al., 2015; Caulfield et al., 2012; Cigolini et al., 2018; Dahren et al., 2012; Deegan et al., 2016; Freundt and Kutterolf, 2019; Geiger et al., 2018; Hollyday et al., 2020; Jeffery et al., 2013; Lai et al., 2018; Lormand et al., 2021; Moussallam et al., 2021, 2019; Namur et al., 2020; Preece et al., 2014; Romero et al., 2022; Ruth and Costa, 2021; Sas et al., 2017; Scruggs and Putirka, 2018; Sheehan and Barclay, 2016).

Existing expressions relating P and/or T to Cpx(±Liq) compositions are generally calibrated on experimental products conducted at known conditions, using a wide variety of equations based on multilinear regressions (e.g. Putirka, 2008, Neave and Putirka, 2017), or most recently, decision-tree machine-learning techniques (e.g., Petrelli et al. 2020, Jorgenson et al. 2021). Although a number of different Cpx-Liq and Cpx-only parametrizations exist (Neave and Putirka, 2017; Nimis, 1999; Petrelli et al., 2020; Putirka, 1999, 2008a; Wang et al., 2021), it is not always clear which parameterization is best, and how much the choice of equation affects geological interpretations. This is particularly true in volcanic arcs, because there has been no detailed evaluation of which thermobarometers behave best in variably hydrous, tholeiitic to calc-alkaline compositions that occur in these settings. This is in contrast to extensive work evaluating thermobarometers in more H_2O-poor tectonic settings such as Iceland (Neave et al., 2019; Neave and Putirka, 2017), and detailed evaluation of the best thermobarometers for alkaline compositions (Masotta et al., 2016; Mollo et al., 2013). Additionally, many existing calibrations are also not parameterized in terms of water contents, and the underlying calibration datasets use a significant number of experiments where H_2O contents are either not measured or are not reported (Wieser et al., 2022a).

The lack of consensus as to the best equations is demonstrated by the wide variety of different equations used by studies published after the major thermobarometry review of Putirka (2008) performing Cpx±Liq thermobarometry in arc magmas (Table 1). As many barometers contain a term for temperature, in natural systems where neither pressure not temperature is known, studies tend to iteratively calculate pressures and temperature using a thermometer and a barometer. This greatly increases the number of possible combinations to perform calculations, to $N_{barometers}$ X $N_{thermometers}$.

Iteration of P and T from Putirka et al., (2003, hereafter P2003) is a popular choice even in recent years, despite the fact that more up-to-date recalibrations of these equations were provided in (Putirka, 2008, hereafter P2008). Eq32c from P2008 is another popular barometer, and has been iterated with a wide variety of different thermometers (Table 1). Another common choice is the iteration of P2008 eq30 or eq31 for pressure with eq33 for temperature. Alternatively, P2008 eq33 (T) has been iterated with the Neave and Putirka (2017, hereafter NP17) barometer, which is interesting given that Neave and Putirka (2017) caution that their barometer may not be applicable to the more hydrous and oxidising conditions found in volcanic arcs.

Cpx-only thermobarometery has been slightly less widely used than Cpx-Liq thermobarometry in volcanic arcs; studies mostly use the two Cpx-only barometers from Putirka (2008, eq32a for H_2O-independent, 32b for H_2O-dependent) iterated with a wide variety of different temperature estimates (e.g. Cpx-only and Cpx-Liq thermometers, Table 1). Three new Cpx-only thermobarometers have recently been published (Jorgenson et al., 2022; Petrelli et al., 2020; Wang et al., 2021), which will likely increase the use of Cpx-only equilibrium in a wide variety of tectonic settings, including volcanic arcs.

The diversity of equations being used in the literature is concerning because these equations give vastly different results for individual Cpx and Cpx-Liq pairs. To demonstrate the magnitude of these differences, we calculate pressures for four experiments from Blatter et al. (2013) performed at 4 kbar and 975-1075 °C using the different combinations of equations highlighted in Table 1, in addition to some of the newest thermobarometers (see also Supporting Fig. 1). Approximate crustal bins are overlain for ease of interpretation. These bins are informed by the crustal thickness compilation of Profeta et al. (2016) as well as convenient cut offs in our new dataset, and are defined as:

- upper crust: $0<P\leq2.51$ kbar
- mid crust: $2.51<P\leq5.1$ kbar
- lower crust: $5.1<P\leq7.6$ kbar
- Moho depths: $7.6<P\leq10.1$ kbar.

We appreciate this exact division into the region of the crust is highly dependent on the total crustal thickness in each arc, however we still feel these are useful divisions for visualizing the performance of barometers in a "typical" continental arc.

Iteration of the Cpx-only thermobarometers of P2008 eq32a-32d (red circles, Fig. 1a) and eq32b-32d (purple dots, Fig. 1a) would suggest crystallization at ~6-8 kbar (lower crust to Moho), while the T-independent Cpx-only barometer of Wang et. (2021) yields pressures of ~ 3-4 kbar (middle crust). Despite these factor of two differences, all Cpx-only pressures overlap within the stated RMSE on the different barometers (Fig. 1a). In contrast, there are very substantial differences in calculated pressures using Cpx-Liq thermobarometers which do not overlap within stated errors (Fig. 1a). For example, the Cpx-Liq thermobarometers of Petrelli et al. (2020) and Jorgenson et al. (2022) suggest crystallization at ~3-5 kbar (mid crust), while iteration of P2008 eq32c for pressure with P2003 for temperature yields pressures in the lower crust (~7.5-11 kbar, brown diamonds), and the default iteration of eq32c in the P2008 spreadsheet yields pressures of 10-12 kbar (brown stars, Fig. 1a). Calculated Cpx-only temperatures show a very wide range (~200˚C) depending on the selected equation, while most Cpx-Liq temperatures lie within ~50-100˚C (Fig. 1b).

Despite these large discrepancies in calculated P and T using different equations, and obvious implications for geological interpretation, only a small proportion of studies applying Cpx-based barometers to natural systems have performed calculations using more than one thermobarometry combination (e.g., Erdmann et al., 2016, Erdmann et al., 2016; Geiger et al., 2018; Sas et al., 2017; Sheehan and Barclay, 2016). In addition to a lack of comparison, there is also a general lack of justification in the literature for why a specific equation was chosen. In many cases, quoted statistics from the paper presenting the thermobarometers are used. For example, some studies appear to select their thermobarometers based on a small quoted SEE/RMSE from the original publication (e.g., Dahren et al., 2012; Preece et al., 2014). However, the way in which RMSE is calculated for these different equations is highly variable, so these statistics are not directly comparable. For example, Putirka et al. (2003) state a RMSE of ±1.7 kbar in their abstract based on the model fit to the calibration dataset (four studies, N=77 experiments). Similarly, Putirka (2008) state an RMSE of ±1.5 kbar for equation 32c based on the calibration dataset (four studies, N=99 experiments). These are the SEEs quoted by Dahren et al., (2012) and Preece et al. (2014) to justify their use of these barometers. However, when Putirka (2008) applied these expressions to all available experimental data (n=1303), Eq 32c has a SEE of ±5 kbar, and Putirka (2003) has a SEE of ±5 kbar for n=324 hydrous experiments, and ±4.8 kbar for 848 anhydrous experiments). Similarly, the SEE=±1.4 kbar commonly quoted by studies using the Neave and Putirka (2017) barometer reflects the fit to the calibration dataset (n=113), while the error on a global regression is ±3.6-3.8 kbar.

Assessing uncertainty using the calibration data can greatly underestimate the true error (as the model has been tuned to those experiments. It is far more statistically robust to assess error using experiments that were not part of the equation calibration (often termed a test dataset), especially when such test datasets share important compositional features with target natural systems. Studies which state the more realistic errors associated with a test dataset in their abstract (e.g., Petrelli et al. 2020) may be less widely used simply because they have quoted a larger error, even though this error is more realistic.

Another issue associated with comparing published statistics, and taking these as representative of the true error in natural systems, is the wide pressure range of calibration and test datasets. For example, Petrelli et al. (2021) compute statistics for their test dataset using experiments conducted at 0-30 kbar, Putirka et al., (2003) from 0-35 kbar, and Neave and Putirka, (2017) from 0-20 kbar. However, it is uncommon that such high pressure Cpx are encountered when examining products from arc volcanoes. Using the compilation of crustal thicknesses from Profeta et al. (2016), all but 2 arcs have Moho depths <45 km (~12 kbar), with only the Northern and Central Volcanic Zone in Chile having Moho depths >50 km (~14-17 kbar). For the test dataset provided with the Cpx-only barometer of Petrelli et al. (2021), if experiments are restricted to those performed at 0-15 kbar, the R^2 value drops from 0.92 to 0.59.

Finally, when testing different barometry equations, most papers input the experimental temperature if the barometer has a temperature term. Similarly, when assessing thermometers, it is common that the experimental pressure is entered to satisfy any pressure terms. However, in natural systems, it is most common that neither pressure nor temperature is known, so a thermometer and a barometer must be selected, and iteratively solved (Table 1). This will increase the error compared to comparisons using experimentally-constrained pressures and temperatures.

Many thermobarometers also contain a term for H_2O. However, the fact that Cpx-only and Cpx-Liq equilibra are not overly sensitive to H_2O means that in most systems, users must estimate a H_2O content (as there are currently no methods to iteratively solve for the three unknowns). Thus, even if errors from iterative calculations on test datasets are assessed, these still may be optimistic compared to the true error associated with application of these methods in natural systems. To get a realistic estimate of the errors associated with thermobarometry when applied to natural systems, we should be assessing their performance on experimental datasets using iterative calculations, over the pressure range of interest, considering any uncertainty in melt H_2O content.

Comparing between different equations for the samples of interest is vital to assess the overall error associated with thermobarometry calculations. Unless one calibration can be robustly selected as the "best" for a given system, the range of P and T from different calibrations may be representative of the true uncertainty in calculated PT conditions. The best equation for a given system may be identified by compiling experiments with similar compositions to the system of interest and assessing which thermobarometry equations best reproduce the experimental values (e.g. Hammer et al., 2016; Neave and Putirka, 2017). Alternatively, if no suitable experimental data exists, insight may be gained by comparing the dataset used to calibrate each thermobarometry equation against the natural compositions of interest to evaluate the degree of extrapolation required (e.g., Wieser et al., 2022b; Wieser et al., 2022c).

These issues and examples demonstrate that there is a clear need for igneous petrologists to be able to directly compare the suitability, accuracy and precision of different thermobarometric expressions in the system of interest. To evaluate the errors associated with calculations of magma storage conditions from Cpx in subduction zones, we compile a new experimental dataset of variably hydrous, tholeiitic to calc-alkaline compositions ranging from basalts to rhyolites. We ensure that none of the test dataset was used to calibrate each model we assess. We calculate a linear regression between experimental P or T (x) and calculated P and T (y), and use five statistical metrics associated with this regression to assess the performance of the equation: the correlation coefficient (R^2), the gradient and intercept of the regression, the root mean square error (RMSE) and the mean absolute error (MAE).

$$RMSE = \sqrt{\frac{1}{N}\sum_{i=1}^{N}(x_i - y_i)^2}$$

$$MAE = \frac{1}{N}\sum_{i=1}^{N}(x_i - y_i)$$

The MAE doesn't have a squared term like the RMSE, so can more easily identify systematic uncertainty. The gradient of the regression also helps identify systematic uncertainty, as does the intercept.

2. METHODS

2.1 ArcPL: a new test dataset for variably hydrous arc magmas

Our new test dataset is mostly comprised of experiments conducted since 2008, when the Library of Experimental Phase Relationship (LEPR) dataset used to calibrate most existing thermobarometers was formally compiled and made available to the community (Hirschmann et al., 2008). These newer experiments are from: Almeev et al., 2013; Alonso-Perez et al., 2009; Andújar et al., 2015; Berndt, 2004; Blatter et al., 2017, 2013; Bogaerts et al., 2006; Cadoux et al., 2014; Costa, 2004; Erdmann and Koepke, 2016; Erdmann et al., 2016; Feig et al., 2010; Firth et al., 2019; Hamada and Fujii, 2008; Husen et al., 2016; Krawczynski et al., 2012; Mandler et al., 2014; Marxer et al., 2022; Melekhova et al., 2015; Mercer and Johnston, 2008; Nakatani et al., 2022; Nandedkar et al., 2014; Neave et al., 2019; Parat et al., 2014; Parman et al., 2011; Pichavant and Macdonald, 2007; Rader and Larsen, 2013; Riker et al., 2015; Rutherford et al., 1985; Sisson et al., 2005; Solaro et al., 2019; Ulmer et al., 2018; and Waters et al., 2021. We also compile a handful of experiments which were not included in the original LEPR compilation, but were conducted prior to 2008 (Berndt, 2004; Rutherford et al., 1985; Sisson et al., 2005). Our new dataset is available in the supporting information.

For other parts of the discussion (e.g., assessing values of equilibrium tests), we also consider experiments conducted on compositions relevant to arc magmas that were present in LEPR

(Baker and Eggler, 1987; Barclay, 2004; Bartels et al., 1991; Berndt et al., 2001; Blatter and Carmichael, 2001; Di Carlo, 2006; Draper and Johnston, 1992, 1992; Feig et al., 2006; Gaetani and Grove, 1998; Grove et al., 2003, 1997, 1982; Hesse and Grove, 2003; Kawamoto, 1996; Martel et al., 1999; Mercer and Johnston, 2008; Moore and Carmichael, 1998). We refer to these experiments as ArcLEPR, and our newly compiled dataset as ArcPL (post-LEPR).

Our ArcPL dataset contains 509 Cpx-Liq pairs which were not used to calibrate the majority of existing thermobarometers. Based on the crustal thickness compilation of Profeta et al., (2016) assuming a crustal density of 2700 kg/m^3, we restrict comparisons to experiments conducted at 0-13 kbar (discarding 4 experiments conducted at 20 kbar). The compositional, pressure (P) and temperature (T) range of this dataset is shown in Fig. 2. While 66% of Cpx-containing experiments in LEPR don't have H_2O contents for experimental glasses, we endeavour to compile as much glass H_2O data as possible for our new dataset. In cases where glass H_2O data was not reported but the experiment was said to be volatile saturated we calculate dissolved H_2O using the solubility model MagmaSat (Ghiorso and Gualda, 2015; implemented in VESIcal; Iacovino et al., 2021) using the quoted experimental P, T and the fluid composition if given (XH_2O). MagmaSat has been shown to provide the best fit to arc magma compositions (Wieser et al., 2022c). Overall, only 9% of our ArcPL dataset is missing H_2O data, and these experiments are not considered when assessing thermobarometers (see Section 2.2).

2.2 Equilibrium Tests

One of the main issues when performing Cpx-Liq thermobarometry in natural systems is selecting which measured Cpx compositions to pair with which liquid compositions. For example, a number of different literature studies have compiled all available whole-rock and glass data, and considered all possible Cpx-Liq matches, discarding pairs which fall outside preferred ranges of several equilibrium tests (Gleeson et al., 2021; Neave et al., 2019; Scruggs and Putirka, 2018). This approach, although popular, is also strongly reliant on having reliable tests by which to assess Cpx-Liq equilibrium. Equilibrium filters have also been applied to experimental datasets when calibrating thermobarometers (Neave and Putirka, 2017). However, a variety of equilibrium tests and cut off values have been proposed, and it is not always clear what values should be used. Thus, we start by evaluating commonly used filters for the ArcPL dataset.

The most widely used equilibrium test assesses partitioning of Fe-Mg between clinopyroxene and liquid ($K_{D,\ Fe-Mg}^{Cpx-Liq}$ abbreviated as K_D). Using LEPR, Putirka (2008) provide an expression (eq35) to calculate K_D solely as a function of temperature:

$$K_{D}=e^{-0.107-\frac{1719}{T\,(K)}}$$

There is ambiguity in the thermobarometry literature as to the best way to compute measured value of K_D from EPMA measurements of Fe-Mg in the Cpx and Liq. Some studies perform the calculation using only Fe^{2+} in the liquid and Fe_T in the Cpx (e.g., Neave et al. 2017, Gleeson et al. 2020), while others use the total amount of Fe (Fe_T) in the liquid (Putirka et al. 2016). It is important to work out which approach works better prior to discarding specific Cpx-Liq pairs, particularly in experiments and natural samples from arcs, which are generally quite rich in Fe^{3+} (Carmichael, 1991; Kelley and Cottrell, 2009).

We calculate the proportion of Fe^{2+} in each experiment using the experimental fO_2 or quoted buffer position and the experimental pressure and temperature, with the equations of Kress and Carmichael (1988) implemented in Thermobar (an open-source Python-based thermobarometry tool, Wieser et al., 2022b). For completeness, although stoichiometric methods estimating Fe^{2+} in minerals are associated with large errors, we also calculate Fe^{2+} in the Cpx using the method of (Lindsley, 1983), and calculate K_D using just Fe^{2+} in both phases.

K_D values are significantly closer to predicted values from Putirka (2008) when Fe_T in both the liquid and Cpx are used (Fig. 3a). When using Fe^{2+} in the liquid and Fe_T in the Cpx (red dots, Fig. 3b), a number of experiments lie outside the ±0.08 window around the predicted value for Putirka (2008), particularly for experiments with >30% Fe^{3+} (Fig. 3d). Using Fe^{2+} in the Liq and Cpx (black squares, Fig. 3b) also results in more experiments failing the equilibrium test compared to using Fe_T for both. The superior performance using just Fe_T is perhaps unsurprising, given that eq35 of Putirka (2008) was calibrated using Fe_T. Thus, we suggest that until equilibrium tests are recalibrated on a substantial volume of experimental data with well constrained Fe^{2+} proportions in liquid (and Cpx), it is best to use Fe_T in both phases for consistency with the calibration of eq35. Using Fe^{2+} in the liquid could lead to more oxidised experiments (or natural samples) being discarded incorrectly (Fig. 3d). It is also interesting that the ±0.03 filter used by many authors (Neave et al., 2019, Scruggs and Putirka, 2018) would exclude a large amount of experimental data (63%), while the ±0.08 value from Putirka (2008) only results in 21% of data being discarded (±0.03 marked by dotted lines, ±0.08 by the grey box on Fig. 3). While deviation from the predicted equilibrium values may represent true disequilibrium in experiments, to retain a reasonably sized dataset, we proceed with the following comparisons using only experiments with measured K_D values that are within ±0.08 of predicted values calculated from eq35 of Putirka (2008).

Wood and Blundy, (1997) also propose an expression:

$$K_D = 0.109 + \frac{0.186}{Mg\#\ Cpx}$$

We find that this performs very poorly, with the offset between calculated and predicted K_D correlating with Cpx Mg# (Supporting Fig. 2).

Comparing the predicted and measured value of the Ca-Tschermak's (CaTs) component is another popular equilibrium test, with most studies using the expression of Putirka (1999) to calculate the predicted CaTs value (e.g., Gleeson et al., 2021; Neave et al., 2019). In the ArcPL dataset, there is a very poor correspondence between predicted and measured CaTs values (Fig. 4a). This is also true for experiments from LEPR conducted on compositions relevant to arc magmas (ArcLEPR, red crosses, Fig. 4a). The discrepancy between predicted and measured values is most apparent at higher measured values of CaTs (Fig. 4a), and correlates most strongly with the Al^{VI} content of the Cpx (Fig. 4b). Al^{VI} in Cpx is one of the key parameters used to calculate the CaTs component:

$$CaTs = Al^{VI} - X_{Na}$$

This means that it is not possible to resolve this offset simply by adding in a term for Al^{VI} in the expression for predicting this component from the liquid component (as this would make it a useless equilibrium test). Clearly, the terms for liquid components, pressure and temperature used in the Putirka (1999) expression to predict the CaTs component are insufficient to account for variation in CaTs in experimental Cpx in hydrous experiments. While the ±0.07 value of Putirka (1999) would result in most experimental pairs being "in equilibrium", use of the ±0.03 value of Neave et al. (2019) would cause a significant number of experimental pairs to be discarded. Given the poor correlation between predicted and measured values, and the correlation of the discrepancy with $Al^{VI,}$ we suggest that CaTs in its current state is not a useful equilibrium test when working with arc magmas.

The measured Enstatite-Ferrosillite (EnFs) component show good agreement with the predicted components using the equation of Mollo et al. (2013) for ArcPL (Fig. 5b) and ArcLEPR (Fig. 5a). Relatively few values lie outside the ±0.05 error window. In contrast, measured Diopside-Hedenbergite (DiHd) values show poor agreement with predicted values using Mollo et al. (2013) for lower temperature experiments, particularly in the ArcPL dataset (Fig. 5c-d). The discrepancy is even worse if DiHd is predicted using Putirka (1999). The overprediction of calculated DiHd values at low temperatures appears to result from the high T-sensitivity of the Mollo expression at these temperatures. To demonstrate this, we calculate predicted DiHd values for 20 randomly-selected Cpx-Liq pairs for temperatures of 750-1400°C. Below ~1000°C, the predicted value rapidly kicks up to higher values (Fig. 5e). When the measured values for these 20 pairs are subtracted from the predicted value, the resulting curves recreate the trend to higher values seen in the whole dataset, indicating that this strong temperature-dependency is the cause of the discrepancy (Fig. 5f). The expressions of Mollo et al (2013) were calibrated using LEPR which contains relatively few experiments at these low temperatures (white squares, Fig. 5f). The lower temperatures of our dataset relative to the calibration range likely result from the higher H_2O contents. These results suggest that care should be taken when applying a DiHd filter to clinopyroxene-liquid pairs that may have crystallized below 900-1000°C, and that this expression likely warrants recalibration with a dataset of lower temperature experiments.

Other equilibrium tests are also of questionable utility. All but one Cpx-Liq pair in ArcPL has a measured CaTi component within the predicted value accounting for the 1σ range of

Putirka (1999, Fig. 6a), but there is a poor correlation between predicted and measured values (indicating it is not a useful test). There is a similarly poor correspondence between predicted and calculated Jd components, with the discrepancy correlating as a function of the Na_2O content of the Cpx (the main component used to calculate Jd, Fig. 6b-c). As for CaTs, this means that recalibration without knowing the Cpx composition is unlikely to be successful.

Overall, these comparisons demonstrate that EnFs, DiHd (for Cpx crystallized at >1000˚C) and K_D calculated using Fe_T with a filter of ±0.08 rather than ±0.03 are currently the most robust tests of equilibrium when assessing possible clinopyroxene-liquid pairs in arc magmas. Because of the range of temperatures in our compiled dataset, we filter our new dataset to include experiments within K_D=±0.08 (using Fe_T) and EnFs (±0.05). We also only include clinopyroxenes with Ca/(Ca+Mg+Ca) on a cation basis between 0.2 and 0.5 (i.e. excluding pigeonites), and cation sums between 3.95 and 4.05. To help alleviate random scatter associated with analytical and experimental imprecision, we only use experiments that measured at least 5 Cpx in each experimental charge (see Wieser et al., 2022a). As many of the thermobarometers assessed here contain a term for H_2O, we also only consider experiments with some form of reported H_2O contents (e.g., SIMS, FTIR or Raman measurements, volatiles-by-difference, or enough information to calculate H_2O using a solubility model). N=106 experimental charges fail the K_D filter, N=74 fail the EnFs filter, N=20 fail the cation sums filter, N=160 fail based on having <5 analyses, and N=45 fail based on no reported H_2O data. Obviously, some experiments fail multiple criteria. Overall, we are left with N=194 experimental charges from the original N=505 which pass all these filters. We use these experiments to assess the best performing thermobarometers in arc magmas.

3. DISCUSSION

3.1. Assessing Cpx-Liq thermobarometers

When estimating temperature from Cpx-Liq equilibrium, iteration of the eq33 of P2008 (for T) with a variety of different barometers (P2008 eq30, P2008 eq32c, and NP17) do a good job of reproducing experimental temperatures in the ArcPL dataset (Fig. 7a-c). The best fit is obtained from iteration of eq33 with Neave and Putirka (2017, Fig. 7a), returning an R^2 value of 0.91, a gradient close to 1 (0.95), and an intercept closest to 0 (80.1°C). This iteration also has the lowest RMSE (32.3°C) and MAE (13.5°C).

Iteration of the thermometer and barometer of Putirka et al. (2003) substantially overestimates temperature, and the discrepancy is correlated with the melt H_2O content (Supporting Fig. 3a). This is unsurprising given this equation doesn't contain a term for H_2O in the liquid (Putirka, 2008), although it has still been widely used since 2008 in hydrous arc magmas (Table 1).

The machine-learning P-independent thermometer of Petrelli et al. (2020) yield slightly worse statistics than P2008 eq33, with the most significant deviation at <1000°C (where it overpredicts temperature, Fig. 7f). Overprediction at low values, and underprediction at high values is common for regression tree methods, as these algorithms will not return a value outside the calibration range of the training dataset. As some of the experiments in ArcPL were used to calibrate the machine learning thermobarometer of Jorgenson et al. (2022), we exclude these data when assessing this equation. For the Jorgenson et al. (2022) thermobarometers, the authors recommend using the median value calculated across all trees, rather than the mean used by Petrelli et al. (2020). For the ArcPL dataset, the median and mean show very similar results for temperature (Supporting Fig. 4), and it is difficult to select which is best. We proceed using the mean value, as this results in slightly less scatter (and less visibly "boxy" results, see Supporting Fig. 4).

It is noteworthy how well the Jorgenson et al. (2022) thermometer behaves given that unlike P2008 eq33 or Petrelli et al. (2020), it does not contain a term for H_2O in the liquid (a parameter which is often poorly constrained in natural systems). Like for Putirka et al. (2003) there is a correlation between the discrepancy between calculated and experimental temperature and H_2O, but the R^2 value and gradient is smaller (R^2=0.2 vs. 0.34, Grad=-8.7 vs. -10.33°C/1 wt% H_2O, Supporting Fig. 3).

Interestingly, the Cpx-saturation thermometer of P2008 (eq34) which only uses the liquid composition also performs well when iterated with NP17, having only a slightly higher RMSE and MAE than eq33, but a gradient closer to 1 (1.02), and a very low intercept (2.7°C, Fig. 8e). The similar performance of eq33 and eq34 raises an interesting question as to how much the temperature calculated with a Cpx-Liq thermometer is sensitive to the Cpx composition, or whether the liquid composition is dominating. Petrelli et al. (2020) examine the relative feature importance of each oxide in their machine learning model, showing that for Cpx-Liq temperatures, the three dominant features are MgO, CaO and H_2O in the liquid. We examine the relative importance of the Cpx vs. Liq term for eq33 of P2008 by pairing each experimental liquid with all of the N=194 Cpx in our filtered dataset. For each liquid, we compare the temperatures obtained from each Cpx to the temperature obtained from the true experimental Cpx. While experimental temperatures vary by 350°C, the temperature only changes by ~±50°C based on the Cpx composition (Supporting Fig. 6). Thus, users should be aware when performing Cpx-Liq thermometry that the thermometer is mostly tracking information on the provided liquid composition, not the Cpx. This is also apparent from the poor performance of Cpx-only thermometers (see Section 3.2).

Cpx-Liq barometers show substantially worse statistics than thermometers (Fig. 8d-f, Fig. 9). None have R^2>0.5, and all predict gradients much less than 1, and intercepts substantially greater than 0. It is difficult to even select what the "best" thermobarometry combination is for predicting pressure. While Petrelli et al. (2020, Fig. 9f) has the highest R^2 value and a good RMSE value (2.2 kbar), the low gradient (0.4) and high intercept (2.92 kbar) show that this barometer substantially overpredicts at low pressures, and underpredicts at high pressures (a common feature of regression tree algorithms as they approach the edges of the calibration range). In fact, experiments conducted at 1 kbar and 10 kbar both yield pressures of ~4 kbar, questioning the ability of this barometer to distinguish between even upper and lower crustal storage (Fig. 9f).

Using a smaller dataset to avoid overlap with the model calibration data, the Jorgeson et al. (2022) barometer using the mean of trees has a slightly higher gradient and lower intercept, and visually returns less of a flat trend than the Petrelli et al. (2020) model (Fig. 9e). Using the median tree value as suggested by the authors (Supporting Fig. 4-5) results in a substantially lower R^2 value (0.27 vs. 0.42), a higher RMSE (2.5 vs. 2 kbar), but a slightly better gradient (0.48 vs. 0.45), and intercept (2.6 vs. 1.8 kbar).

Iteration of NP17 with P2008 eq33 returns disappointing R^2, RMSE and MAE values (Fig. 9a), but the gradient is substantially higher than for machine learning algorithms (0.64) and the intercept much closer to zero (-0.27 kbar). Thus, while there is a lot of random error, this barometer shows less systematic error. Iteration of Eq31-Eq33 (Fig 9c), Eq32c-Eq33 (Fig 9d) and P&T from P2003 (Fig. 8d) yield very flat trends with disappointing statistics, and very little difference in calculated pressure between 1 kbar and 10 kbar experiments.

By default, when the spreadsheet of P2008 is downloaded (up until 2022), the first cell in the column for Eq32c takes its temperature from iteration of P2008 eq34 and P1996 EqP1. The rest of the cells iterate P1996 EqP1-EqT2. Many studies have used this set up by default (Table 1), although we do not know how they dragged the formula down (e.g. whether the first cell or subsequent cell formula was used for most calculations). Regardless, this combination of thermobarometers performs extremely poorly, overpredicting pressure by an average of 3.6 to 4.5 kbar, with an intercept of ~5.1-5.8 kbar (Fig. 8e, Supporting Fig. 7). Studies using this combination (Table 1) have likely greatly overestimated storage pressure.

3.1.1. Sensitivity of Cpx-Liq thermobarometry to H_2O

For the comparisons shown in Fig. 7-9, experimental H_2O contents were used for calculations. However, in most natural systems, the H_2O content of the melt is highly uncertain, particularly in volcanic systems with no melt inclusion data (e.g., a paucity of rapidly-quenched tephra, or at understudied volcanoes). Thus, we investigate how much changing H_2O influences the calculated temperature (Fig. 10) and pressure (Fig. 11), to give insight into the additional sources of uncertainty affecting calculations in variably hydrous arc systems.

We randomly select 41 Cpx-Liq pairs from ArcPL. For each of these pairs, we perform calculations at the experimental H_2O, and then perturb H_2O by ±3 wt%, which represents a reasonable uncertainty on the water content of arc systems (where melt inclusion measurements of H_2O generally vary between ~0-6 wt% H_2O; Plank et al., 2013). For each discrete H_2O content, we take the calculated temperature and pressure, and subtract the value calculated using the experimental H_2O content. We do not show results performed using negative water contents. The variation in H_2O for each Cpx-Liq pair is shown as a single line, stretching either side of a black circle showing the experimental H_2O content (where the difference between the perturbed and experimental calculation is 0, Fig. 10-11).

Different calibration approaches show different sensitivity to H_2O perturbations. The regression-tree nature of the Cpx-Liq thermometer of Petrelli et al. (2020) means that it shows complex sensitivity to H_2O (blue lines, Fig. 10a). At lower H_2O contents, the thermometer is extremely sensitive, with temperatures decreasing by as much as 70°C for a ~2 wt% increase in H_2O. At higher H_2O contents, calculated temperature changes very little, and in some cases, actually increases with increasing H_2O. In contrast, using experimental pressures, P2008 eq33 shows a clear decline in calculated temp with H_2O, with much smaller differences between samples than for Petrelli et al. (2020, Fig. 10b). When eq33 is iterated with P from eq30 instead of using experimental pressures, the temperature still drops (Fig. 10c), but there is a smaller decrease per unit increase in H_2O than in Fig. 10b. There is also a reasonably similar drop with increasing H_2O for eq33 iterated with NP17 (Fig. 10d). Excluding Petrelli et al. (2022) uncertainty in H_2O of only 1 wt% corresponds to an uncertainty in temperature of 10°C.

Performing the same exercise for Cpx-Liq barometers, we find that Petrelli et al. (2020) shows erratic behaviour, with calculated pressure decreasing with increasing H_2O until ~6 wt%, then increasing again (Fig. 11a). However, the change for all samples is relatively small (<1 kbar). When using experimental temperatures, eq30, eq31, and eq32c show an increase in calculated pressure with increasing H_2O, and all samples show the same gradient (because the H_2O term is multiplied by a constant in each of these equations, Fig. 11b). In contrast, these three barometers show very different behaviour when iterated with eq33, reflecting the fact that temperature and pressure are both affected by H_2O, and they are being iteratively solved (Fig. 11c). In all cases, the change in calculated pressure with changing H_2O for iterative calculations is more subtle than when using experimental temperatures. This is because increasing H_2O decreases the temperature, which decreases the pressure, counteracting the effect of increasing H_2O increasing the pressure. The effect of changing temperature is so dominant for eq31, that iterative calculations see a decrease in pressure with increasing H_2O (although the effect is relatively subtle). Iteration of eq30 and eq33 is the most sensitive to H_2O, with uncertainty of just 1 wt% in H_2O results in an uncertainty in pressure of 0.26-0.63 kbar. The NP17 barometer has no H_2O term, but iterative calculations using this barometer can still be H_2O-sensitive if a H_2O-sensitive thermometer is used, because the barometer is temperature sensitive. Iteration with eq33 results in a relatively small H_2O effect (0.09 kbar per 1 wt% H_2O, Fig. 11d).

Given the fact temperature and pressure sensitivity is highly dependent on the choice of equations to iterate, we suggest that in systems where H_2O is not very well constrained, users should propagate uncertainties using methods similar to those here, to assess the possible systematic uncertainty introduced by H_2O terms in equations.

3.2. Assessing suitable Cpx-only thermobarometers

Given the poor behaviour of many Cpx-Liq equilibrium tests in arc compositions, and the difficulty identifying liquid compositions in arcs where many erupted materials are highly crystalline, it would be advantageous to be able to use Cpx-only thermobarometers to deduce magma storage conditions. We assess the performance of the Cpx-only thermobarometers from Putrirka (2008), Petrelli et al. (2020), Jorgenson et al. (2022) and Wang et al. (2021). None of the experiments in our ArcPL test dataset appear in the calibration datasets of Putirka (2008) and Petrelli et al. (2020). Wang et al. (2021) include the experiments of Berndt (2004) and Husen et al. (2016). The calibration dataset of Jorgenson et al. (2022) has substantial overlap with our test dataset (Almeev et al., 2013; Berndt, 2004; Feig et al., 2010; Husen et al., 2016; Krawczynski et al., 2012; Melekhova et al., 2015; Nandedkar et al., 2014; Parat et al., 2014; Ulmer et al., 2018). To obtain the largest possible test dataset here, we exclude these overlapping experiments when testing each thermobarometer only in Fig. 12-13. For fair comparisons between the best barometers in Fig. 14, we only use data which isn't present in any of the calibration datasets.

Putirka (2008) present a number of Cpx-only thermobarometers. P2008 eq32d is a P-sensitive, H_2O-independent Cpx-only thermometer. There is also a subsolidus version of eq32d. P2008 eq32a is a T-sensitive barometer which uses only uses the composition of the Cpx, while eq32b also requires users to specify the H_2O content of the liquid. Petrelli et al. (2020) present a Cpx-only barometer calibrated using an extra trees regression (with no H_2O term), but do not present a Cpx-only thermometer. Jorgenson et al. (2022) present a Cpx-only thermometer and barometer, neither of which include a H_2O term. Finally, Wang et al. (2021) present a thermometer (eq2) which has a H_2O term but is P-independent, and a barometer (eq1) which has a T and H_2O term.

When P2008 eq32d (T) is iterated with eq32a or eq32b (P), almost the same temperature is returned for all samples (Fig. 12a-b). This iterated thermometer overpredicts temperatures by >200°C for the lower temperature experiments. The subsolidus version performs slightly better (lower RMSE and MAE), but greatly underestimates most temperatures (Fig. 12c-d). Putirka (2008) do note that eq32d underestimates temperatures in hydrous systems, and indeed we find a correlation between the discrepancy (Exp-Calc T) and H_2O in the liquid (eq32d-32b, R^2=0.47, ~-26°C/1 wt%, eq32d-32a: R^2=0.35, ~-20°C/1 wt%, Supporting Fig. 8). Thus, we do not recommend using either of these Cpx-only thermometers in hydrous arc magmas.

The Jorgenson et al. (2022) thermometer also overpredicts temperature (Fig. 12e), and the discrepancy correlates with H_2O (R^2=0.48, ~-28°C/1 wt%, Supporting Fig. 8). The median and mean of trees show similarly poor performance (Supporting Fig. 9-10).

The Wang et al. (2021) thermometer performs the best (Fig. 12f), which is perhaps unsurprising given that this is the only Cpx-only thermometer which contains a H_2O term. However, it is worth noting that this equation was only calibrated using liquids with SiO_2 contents <60 wt% (e.g. basalts and basaltic-andesites). We find that the discrepancy increases greatly at higher SiO_2 contents (overpredicting by 200-300°C for the most silicic compositions in our test dataset, Supporting Fig. 11a). When only experimental Cpx crystallized in liquids with SiO_2<60 wt% are considered, this thermometer performs much better (Supporting Fig. 11b), with an R^2=0.61, and RMSE=40.5°C. The main problem is that it is difficult to identify from Cpx compositions alone whether a given crystal formed from a liquid with SiO_2>60 wt%. We do not find any robust correlations between Cpx composition and the discrepancy that could be used to apply this filter in natural systems. Thus, the Wang et al. (2021) thermometer needs to be used with extreme care in systems where Cpx may have crystallized from higher SiO_2 liquids. Overall, it is clear from these comparison that Cpx compositions grown from arc magmas do not hold sufficient temperature information without an independent estimate on the melt H_2O content from which they grew. Even when H_2O is included in the regression, Cpx-only is not a very precise thermometer.

All Cpx-only barometers have intercepts >0, and gradients <1 (Fig. 13), which was also seen for Cpx-Liq barometers. These statistics indicate that all equations yield anomalously high pressures for low P experiments (e.g., an intercept of 3.2 kbar for eq32d-eq32a, 4.5 kbar for eq32d- eq32b, and 2.8 kbar for Petrelli et al. 2020). Most thermobarometers also underpredict high pressure experiments (shown by the low gradient). The Wang et al. (2021) barometer has a lower intercept (1.7 kbar), but also a reasonably low gradient, so while it does a reasonable job at low pressures, it underestimates all experiments at > 4 kbar (Fig. 13d). The Jorgenson et al. (2022) barometer is certainly the best of a bad lot, with a low intercept (1.77

kbar), high gradient relative to other expressions (0.61), and a low RMSE (1.8 kbar) and MAE (0.19 kbar, Fig. 13f). As for Cpx-Liq, if the median tree is used rather than the mean, the R^2 and RMSE value is worse, but the gradient and intercept slightly better (Supporting Fig. 9).

When Petrelli et al. (2020) is applied to the same small dataset used to assess Jorgenson et al. (2022), it is clear that Jorgenson performs slightly better (Fig. 13f vs. g). This is likely because Jorgenson et al (2022) have more hydrous arc magma like compositions in their calibration dataset. Using the median tree, rather than the mean used by Petrelli et al. (2020) isn't accompanied by any obvious improvement, for either Cpx-only or Cpx-Liq (Supporting Fig. 5, 10)

Jorgenson et al. (2022) also suggest that the standard deviation of all the estimates from a regression tree could be used to help filter out poor results in machine-learning based thermobarometers, which may help improve the performance of their thermobarometers further. Unfortunately, we find that there is no correlation between the discrepancy between experiment and calculated pressure (or temperature), and the standard deviation of all trees (Supporting Fig. 12). We also find no correlation applying this same method to the Petrelli et al. (2020) barometer. Thus, at present, it does not seem that applying such a filter is useful.

3.2.1. Sensitivity of Cpx-Liq thermobarometry to H_2O

It is unlikely that H_2O contents will be precisely known when applying Cpx-only thermobarometry to natural systems (unless melt inclusions in Cpx are analysed). As for Cpx-Liq, we assess the sensitivity of different equation combinations to H_2O, to give insights into the additional uncertainties when applying these equations to natural systems. The Wang et al (2021) Cpx-only thermometer (eq2) is extremely sensitive to H_2O, with calculated temperature decreasing by 23.4°C per 1 wt% H_2O added (Fig. 14a). While eq32d doesn't have a H_2O term itself, eq32b does, meaning that when these are iterated, calculated temperature actually increases with H_2O (because H_2O changes pressure, which changes temperature). Fortunately, this seemingly spurious effect arising from iteration is quite subtle, with temperature only increasing by ~4-5.6°C per 1 wt% H_2O added (Fig. 14a).

Of the Cpx-only barometers discussed here, only eq32b contains a H_2O term. Calculated temperatures increase quite dramatically with added H_2O (mean increase of +0.61 kbar per 1 wt% H_2O, Fig. 14b). This represents an additional source of error when applying this equation in natural systems, and should be propagated to obtain an uncertainty window.

3.3. What utility does Cpx-Liq thermobarometry have in natural systems

Our new test dataset shows that Cpx-Liq thermometers are reasonably successful, although this is mostly attributed to the temperature information held in the liquid (shown by the similar performance of Liq-only and Cpx-Liq thermometers, and poor performance of Cpx-only thermometers). Cpx-only thermometers are very unreliable in hydrous arc magmas, and even when a temperature term is included, they are still not very accurate or precise (Fig. 12f), particularly for more silicic compositions.

Cpx-Liq and Cpx-only barometers are associated with large systematic and random errors. Systematic error is the reason why many equations have gradients and intercepts substantially different from the 1:1 line, and may arise from the fact that hydrous experiments are relatively poorly represented in the LEPR calibration dataset used to calibrate many barometers. Sources of random error indicated by large RMSEs and low R^2 values are discussed in detail in Wieser et al. (2022a). Briefly, they suggest that a substantial amount of random error is introduced because of low analytical precision during analyses of minor components such as Na_2O in experimental Cpx. We have attempted to mitigate the effect of this by only using experiments which measured >5 Cpx, but barometers still show poor performance. Thus, we investigate whether averaging multiple different experiments conducted at similar pressures can help eliminate random error further (following Putirka et al. 1996).

We specifically investigate the two best behaving Cpx-only barometers (Wang et al. 2021 and Jorgenson et al. 2022, Fig. 15a-b), and the two best-behaving Cpx-Liq barometers (Iteration of P2008 eq33 and Neave and Putirka, 2017, and Jorgenson et al. 2022, Fig. 15c-d). In order to compare these expressions, we only use experiments which do not appear in the calibration datasets of any of these 4 models. We use the approximate crustal bins discussed in Section 1 for averaging. For each bin, we take the mean of the experimental pressure, and the mean of the calculated pressure, and plot this as symbol with an error bar showing the 1σ of the averaged experiments (Fig. 15a).

The Tukey pairwise test can be used to assess whether the mean of calculated pressures for different crustal bins are statistically distinct at $p=0.05$. Full statistics are given in Supporting Fig. 13. For the Wang et al. (2021) Cpx-only barometer, all bins except the mid and lower crustal bin ($p=0.91$), and lower and Moho crustal bin ($p=0.23$) can be distinguished from one another. It is clear from Fig.15 a that this barometer works very well at <5 kbar (with the upper and mid crustal bin averages lying very close to the 1:1 line), and then its performance tails off, predicting too low pressures at >5 kbar.

For the Jorgenson et al. (2022) Cpx-only barometer, the 1σ values on all bin averages overlap with the 1:1 line, so in a natural system, the mean and the error bar on a series of averaged natural Cpx would overlap with the true value (Fig. 15b). However, as for Wang et al. (2021), the mid and lower crustal ($p=0.29$) and lower crustal and Moho bin ($p=0.97$) cannot be distinguished at $p=0.05$.

Cpx-Liq pressures calculated by iterating P2008 eq33 and NP17 only produces upper and middle crust bin averages that overlap with the 1:1 within ±1σ (Fig. 15c). The mid and lower (p=0.37), mid and Moho (p=0.85) and lower and Moho (p=0.47) are indistinguishable. Thus, this barometer can only confidently identify whether a Cpx formed in the upper crust or not.

Bin averages from Cpx-Liq pressures using Jorgenson et al. (2022) are a less good match to the 1:1 line vs. Cpx-only pressures (Fig. 15d vs b). The upper and Moho bins lie more than ±1σ off the 1:1 line, although only the lower and Moho bin averages are statistically indistinguishable.

Overall, these comparisons show that even when substantial numbers of experiments are averaged, Cpx-only and Cpx-Liq barometery can only really help to pinpoint broad areas of crustal storage. This means they can help answer research questions investigating whether specific magma compositions are stored in the upper, mid or lower crust/lithospheric mantle. However, at present, Cpx-based barometers do not have sufficient resolution to identify closely-space magma chambers, or determine pressures with a resolution <2-3 kbar (~<10 km). Commonly quoted standard error estimates of <2 kbar are misleading, and not representative of the errors associated with the application of these methods in natural systems (where P and T must be iteratively solved, and compositions are not the exact ones used to calibrate the model).

Interestingly, Cpx-only barometers behave just as well, if not slightly better than Cpx-Liq barometers in arc magmas. Thus, it seems the additional uncertainty and effort associated with identifying equilibrium liquids in natural systems is likely not justified (although liquid compositions are certainly required to obtain reliable temperature information). The best barometers are the Cpx-only barometers of Wang et al. (2021) and Jorgenson et al. (2022), although these still have very large RMSE, and struggle to distinguish between lower crust and Moho pressures in our experimental dataset. When applied in nature, Cpx-only and Cpx-Liq barometers will likely perform even more poorly than for these experiments, because of uncertainty in H_2O contents.

4. FUTURE DIRECTIONS

The poor performance of Cpx-based barometers (and thermometers) in volcanic arcs is disappointing, as thermobarometry is often one of the only available petrological tools for investigating magma plumbing system geometries; many arc volcanoes have no rapidly quenched tephra for melt inclusion work, and Amp-only barometry is equally problematic (Erdmann et al., 2014). Moving forwards, recalibration of Cpx-based barometry based on higher quality experimental data using longer count times for minor elements such as Na, and more analyses per experiment may help to provide a new dataset upon which to recalibrate the next generation of thermobarometers (see Wieser et al. 2022a). However, without access to such a high-quality dataset, it is difficult to determine how much improvement this may yield, and performance will always be restricted by the relatively weak thermodynmaic relationship between mineral components and pressure (Putirka, 2008).

It is also worth considering the Cpx-based thermobarometry is fundamentally limited by the fact we are trying to calculate pressure and temperature-sensitive components based on EPMA analyses of minerals and melts. Tommasini et al. (2022) examine natural Cpx crystals from Popocat´epetl Volcano, and show that mineral components (e.g. Jd) calculated from XRD-informed site assignments differ greatly from the routines used by Neave and Putirka (2017) and P2008 using EPMA data alone. It is very plausible that if the Cpx components could be calculated more precisely and accurately, the performance of thermobarometers would greatly increase.

Additionally, it has been suggested that the presence of Fe^{3+} in Cpx from more oxidised melts stabilizes an aegirine component ($NaFe^{3+}SiO_6$), which convolutes the relationship between pressure and the clinopyroxene Jd component (see Blundy et al., 1995; Neave et al., 2019; Neave and Putirka, 2017 for further discussion). For tholeiitic magmas, Neave et al. (2019) conclude that the aegirine component is not a significant issue, and that perhaps Fe^{3+} is incorporated as a Ca-Al bearing CaFe Tschermak's component. Our dataset, spanning a wider range of fO_2 that of Neave and Putirka (2017) and Neave et al. (2019), shows no clear correlation between the discrepancy between calculated and predicted pressure, and the calculated Fe^{3+} proportion in the liquid (from the experimental fo2), or the proportion of Fe^{3+} predicted in the Cpx using the parameterization in the spreadsheet of Putirka (2008) after Lindsley, (1983). However, stoichometric techniques to calculate Fe^{3+} in Cpx are "misleading, inconsistent, and inaccurate" (Dyar et al., 1989), and extremely sensitive to propagated uncertainties from the measurement of other cations (McCanta et al., 2018; Sobolev et al., 1999). While Mössbauer spectroscopy offers high precision detection of Fe^{3+}, it is a bulk analysis method requiring >100 mg of sample, so cannot be applied to the vast majority of experimental products (Rudra, 2021). XANES measurements are challenging, and must take crystal orientation into account because the anisotropy of Cpx to x-ray absorption means orientation must also be taken into account (McCanta et al., 2018; Rudra, 2021). Extensive work determining Fe^{3+} proportions for Cpx in different experimental charges at different redox conditions by XANES, combined with more accurate determination of mineral components, is likely needed to investigate why barometers seem to perform more poorly in arc magmas than tholeiitic magmas (e.g. Neave et al. 2019).

4. CONCLUSION

Our evaluation of a new dataset of hydrous experiments filtered for K_D and EnFs disequilibrium, cation sums, and number of analyses per experiment, provides new insights into the best thermobarometry calibrations to use when investigating pressures and temperatures in hydrous arc magmas using Cpx-liquid and Cpx alone. We show that the Cpx-Liq thermometers from Petrelli et al. (2020), Jorgenson et al. (2022), and P2008 eq33 all perform well, and can give important insights into magma storage temperatures. However, the majority of temperature information is stored in the liquid, rather than the Cpx. In contrast, Cpx-only thermometers which do not have a term for H_2O in the liquid perform very poorly indeed, substantially overestimating temperatures for hydrous magmas (e.g. P2008 eq32d, Jorgenson et al. 2022). Only the expression of Wang et al. (2021) which includes a H_2O term shows a reasonable correspondence between experimental and calculated temperatures, and only for Cpx grow in liquids with SiO_2<60 wt%.

Cpx-Liq and Cpx-only barometers all behave poorly, with large random and systematic errors. Even the best barometers only just manage to distinguish between storage zones ~2-3 kbar (or ~ 10 km) apart. Some commonly-used barometers behave extremely poorly, overpredicting pressures by ~4 kbar (Fig. 8e). Thus, with present calibrations, Cpx-only barometry can only provide broad insights into magma storage depths, and does not have sufficient resolution to identify reservoirs located close together, or robustly distinguish subtle differences in magma storage within an eruptive sequence. Substantial experimental work is required to obtain precise (or even accurate) pressures from Cpx compositions in volcanic arcs. Given the importance of determining magma storage depths in arcs (Hilley, 2022), this should be a key focus of the experimental and petrological community moving forwards.

Acknowledgements

PW thanks helpful conversations with Matt Gleeson and Keith Putirka. This contribution was supported by funding from National Science Foundation grants 1948862 and 1949173 to AJRK and CBT, and start up funds to PW from UC Berkeley.

Data Availability Statement

The excel file containing the new experimental dataset (ArcPL), along with the Jupyter Notebooks used to make every figure can be found on Penny Wieser's GitHub https://github.com/PennyWieser/BarometersBehavingBadly_PartII. Upon acceptance, this will be archived on Zenodo.

5. REFERENCES

Almeev, R.R., Holtz, F., Ariskin, A.A., Kimura, J.-I., 2013. Storage conditions of Bezymianny Volcano parental magmas: results of phase equilibria experiments at 100 and 700 MPa. Contrib Mineral Petrol 166, 1389–1414. https://doi.org/10.1007/s00410-013-0934-x

Alonso-Perez, R., Müntener, O., Ulmer, P., 2009. Igneous garnet and amphibole fractionation in the roots of island arcs: experimental constraints on andesitic liquids. Contrib Mineral Petrol 157, 541–558. https://doi.org/10.1007/s00410-008-0351-8

Andújar, J., Scaillet, B., Pichavant, M., Druitt, T.H., 2015. Differentiation Conditions of a Basaltic Magma from Santorini, and its Bearing on the Production of Andesite in Arc Settings. Journal of Petrology 56, 765–794. https://doi.org/10.1093/petrology/egv016

Auer, A., White, J., Nakagawa, M., Rosenberg, M., 2013. Petrological record from young Ruapehu eruptions in the 4.5 ka Kiwikiwi Formation, Whangaehu Gorge, New Zealand. New Zealand Journal of Geology and Geophysics 56, 121–133. https://doi.org/10.1080/00288306.2013.796998

Baker, D.R., Eggler, D.H., 1987. Compositions of anhydrous and hydrous melts coexisting with plagioclase, augite, and olivine or low-Ca pyrxene from 1 atm to 8 kbar: Application to the Aleutian volcanic center of Atka. American Mineralogist 72.

Barclay, J., 2004. A Hornblende Basalt from Western Mexico: Water-saturated Phase Relations Constrain a Pressure-Temperature Window of Eruptibility. Journal of Petrology 45, 485–506. https://doi.org/10.1093/petrology/egg091

Bartels, K.S., Kinzler, R.J., Grove, T.L., 1991. High pressure phase relations of primitive high-alumina basalts from Medicine Lake volcano, northern California. Contr. Mineral. and Petrol. 108, 253–270. https://doi.org/10.1007/BF00285935

Belousov, A., Belousova, M., Auer, A., Walter, T.R., Kotenko, T., 2021. Mechanism of the historical and the ongoing Vulcanian eruptions of Ebeko volcano, Northern Kuriles. Bull Volcanol 83, 4. https://doi.org/10.1007/s00445-020-01426-z

Berndt, J., 2004. An Experimental Investigation of the Influence of Water and Oxygen Fugacity on Differentiation of MORB at 200 MPa. Journal of Petrology 46, 135–167. https://doi.org/10.1093/petrology/egh066

Berndt, J., Holtz, F., Koepke, J., 2001. Experimental constraints on storage conditions in the chemically zoned phonolitic magma chamber of the Laacher See volcano. Contrib Mineral Petrol 140, 469–486. https://doi.org/10.1007/PL00007674

Blatter, D.L., Carmichael, I.S.E., 2001. Hydrous phase equilibria of a Mexican high-silica andesite:A candidate for a mantle origin? Geochimica et Cosmochimica Acta 65, 4043–4065. https://doi.org/10.1016/S0016-7037(01)00708-6

Blatter, D.L., Sisson, T.W., Hankins, W.B., 2017. Voluminous arc dacites as amphibole reaction-boundary liquids. Contrib Mineral Petrol 172, 27. https://doi.org/10.1007/s00410-017-1340-6

Blatter, D.L., Sisson, T.W., Hankins, W.B., 2013. Crystallization of oxidized, moderately hydrous arc basalt at mid- to lower-crustal pressures: implications for andesite genesis. Contrib Mineral Petrol 166, 861–886. https://doi.org/10.1007/s00410-013-0920-3

Blundy, J.D., Falloon, T.J., Wood, B.J., Dalton, J.A., 1995. Sodium partitioning between clinopyroxene and silicate melts. J. Geophys. Res. 100, 15501–15515. https://doi.org/10.1029/95JB00954

Bogaerts, M., Scaillet, B., Auwera, J.V., 2006. Phase Equilibria of the Lyngdal Granodiorite (Norway): Implications for the Origin of Metaluminous Ferroan Granitoids. Journal of Petrology 47, 2405–2431. https://doi.org/10.1093/petrology/egl049

Cadoux, A., Scaillet, B., Druitt, T.H., Deloule, E., 2014. Magma Storage Conditions of Large Plinian Eruptions of Santorini Volcano (Greece). Journal of Petrology 55, 1129–1171. https://doi.org/10.1093/petrology/egu021

Carmichael, I.S.E., 1991. The redox states of basic and silicic magmas: a reflection of their source regions? Contr. Mineral. and Petrol. 106, 129–141. https://doi.org/10.1007/BF00306429

Cassidy, M., Watt, S.F.L., Talling, P.J., Palmer, M.R., Edmonds, M., Jutzeler, M., Wall-Palmer, D., Manga, M., Coussens, M., Gernon, T., Taylor, R.N., Michalik, A., Inglis, E., Breitkreuz, C., Le Friant, A., Ishizuka, O., Boudon, G., McCanta, M.C., Adachi, T., Hornbach, M.J., Colas, S.L., Endo, D., Fujinawa, A., Kataoka, K.S., Maeno, F., Tamura, Y., Wang, F., 2015. Rapid onset of mafic magmatism facilitated by volcanic edifice collapse: MAFIC MAGMATISM FACILITATED BY VOLCANIC EDIFICE COLLAPSE. Geophys. Res. Lett. 42, 4778–4785. https://doi.org/10.1002/2015GL064519

Caulfield, J.T., Turner, S.P., Smith, I.E.M., Cooper, L.B., Jenner, G.A., 2012. Magma Evolution in the Primitive, Intra-oceanic Tonga Arc: Petrogenesis of Basaltic Andesites at Tofua Volcano. Journal of Petrology 53, 1197–1230. https://doi.org/10.1093/petrology/egs013

Cigolini, C., Taticchi, T., Alvarado, G.E., Laiolo, M., Coppola, D., 2018. Geological, petrological and geochemical framework of Miravalles-Guayabo caldera and related lavas, NW Costa Rica. Journal of Volcanology and Geothermal Research 358, 207–227. https://doi.org/10.1016/j.jvolgeores.2018.05.013

Costa, F., 2004. Petrological and Experimental Constraints on the Pre-eruption Conditions of Holocene Dacite from Volcan San Pedro (36 S, Chilean Andes) and the Importance of Sulphur in Silicic Subduction-related Magmas. Journal of Petrology 45, 855–881. https://doi.org/10.1093/petrology/egg114

Dahren, B., Troll, V.R., Andersson, U.B., Chadwick, J.P., Gardner, M.F., Jaxybulatov, K., Koulakov, I., 2012. Magma plumbing beneath Anak Krakatau volcano, Indonesia: evidence for multiple magma storage regions. Contrib Mineral Petrol 163, 631–651. https://doi.org/10.1007/s00410-011-0690-8

Deegan, F.M., Whitehouse, M.J., Troll, V.R., Budd, D.A., Harris, C., Geiger, H., Hålenius, U., 2016. Pyroxene standards for SIMS oxygen isotope analysis and their application to Merapi volcano, Sunda arc, Indonesia. Chemical Geology 447, 1–10. https://doi.org/10.1016/j.chemgeo.2016.10.018

Di Carlo, I., 2006. Experimental Crystallization of a High-K Arc Basalt: the Golden Pumice, Stromboli Volcano (Italy). Journal of Petrology 47, 1317–1343. https://doi.org/10.1093/petrology/egl011

Draper, D.S., Johnston, A.D., 1992. Anhydrous PT phase relations of an Aleutian high-MgO basalt: an investigation of the role of olivine-liquid reaction in the generation of arc high-alumina basalts. Contr. Mineral. and Petrol. 112, 501–519. https://doi.org/10.1007/BF00310781

Dyar, M.D., McGuire, J., Ziegler, R., 1989. Redox equilibria and crystal chemistry of coexisting minerals from spinel lherzolite mantle xenoliths. American Mineralogist 74, 969–980.

Erdmann, M., Koepke, J., 2016. Silica-rich lavas in the oceanic crust: experimental evidence for fractional crystallization under low water activity. Contrib Mineral Petrol 171, 83. https://doi.org/10.1007/s00410-016-1294-0

Erdmann, S., Martel, C., Pichavant, M., Bourdier, J.-L., Champallier, R., Komorowski, J.-C., Cholik, N., 2016. Constraints from Phase Equilibrium Experiments on Pre-eruptive Storage Conditions in Mixed Magma Systems: a Case Study on Crystal-rich Basaltic Andesites from Mount Merapi, Indonesia. J. Petrology 57, 535–560. https://doi.org/10.1093/petrology/egw019

Erdmann, S., Martel, C., Pichavant, M., Kushnir, A., 2014. Amphibole as an archivist of magmatic crystallization conditions: problems, potential, and implications for inferring magma storage prior to the paroxysmal 2010 eruption of Mount Merapi, Indonesia. Contrib Mineral Petrol 167, 1016. https://doi.org/10.1007/s00410-014-1016-4

Feig, S.T., Koepke, J., Snow, J.E., 2010. Effect of oxygen fugacity and water on phase equilibria of a hydrous tholeiitic basalt. Contrib Mineral Petrol 160, 551–568. https://doi.org/10.1007/s00410-010-0493-3

Feig, S.T., Koepke, J., Snow, J.E., 2006. Effect of water on tholeiitic basalt phase equilibria: an experimental study under oxidizing conditions. Contrib Mineral Petrol 152, 611–638. https://doi.org/10.1007/s00410-006-0123-2

Firth, C., Adam, J., Turner, S., Rushmer, T., Brens, R., Green, T.H., Erdmann, S., O'Neill, H., 2019. Experimental constraints on the differentiation of low-alkali magmas beneath the Tonga arc: Implications for the origin of arc tholeiites. Lithos 344–345, 440–451. https://doi.org/10.1016/j.lithos.2019.07.008

Freundt, A., Kutterolf, S., 2019. The long-lived Chiltepe volcanic complex, Nicaragua: magmatic evolution at an arc offset. Bull Volcanol 81, 60. https://doi.org/10.1007/s00445-019-1321-x

Gaetani, G.A., Grove, T.L., 1998. The influence of water on melting of mantle peridotite. Contributions to Mineralogy and Petrology 131, 323–346. https://doi.org/10.1007/s004100050396

Geiger, H., Troll, V.R., Jolis, E.M., Deegan, F.M., Harris, C., Hilton, D.R., Freda, C., 2018. Multi-level magma plumbing at Agung and Batur volcanoes increases risk of hazardous eruptions. Sci Rep 8, 10547. https://doi.org/10.1038/s41598-018-28125-2

Ghiorso, M.S., Gualda, G.A.R., 2015. An H2O–CO2 mixed fluid saturation model compatible with rhyolite-MELTS. Contrib Mineral Petrol 169, 53. https://doi.org/10.1007/s00410-015-1141-8

Gleeson, M.L.M., Gibson, S.A., Stock, M.J., 2021. Upper Mantle Mush Zones beneath Low Melt Flux Ocean Island Volcanoes: Insights from Isla Floreana, Galápagos. Journal of Petrology 61, egaa094. https://doi.org/10.1093/petrology/egaa094

Grove, T.L., Donnelly-Nolan, J.M., Housh, T., 1997. Magmatic processes that generated the rhyolite of Glass Mountain, Medicine Lake volcano, N. California. Contributions to Mineralogy and Petrology 127, 205–223. https://doi.org/10.1007/s004100050276

Grove, T.L., Elkins-Tanton, L.T., Parman, S.W., Chatterjee, N., M�ntener, O., Gaetani, G.A., 2003. Fractional crystallization and mantle-melting controls on calc-alkaline differentiation trends.

Contributions to Mineralogy and Petrology 145, 515–533. https://doi.org/10.1007/s00410-003-0448-z

Grove, T.L., Gerlach, D.C., Sando, T.W., 1982. Origin of calc-alkaline series lavas at Medicine Lake Volcano by fractionation, assimilation and mixing. Contr. Mineral. and Petrol. 80, 160–182. https://doi.org/10.1007/BF00374893

Hamada, M., Fujii, T., 2008. Experimental constraints on the effects of pressure and H2O on the fractional crystallization of high-Mg island arc basalt. Contrib Mineral Petrol 155, 767–790. https://doi.org/10.1007/s00410-007-0269-6

Hammer, J., Jacob, S., Welsch, B., Hellebrand, E., Sinton, J., 2016. Clinopyroxene in postshield Haleakala ankaramite: 1. Efficacy of thermobarometry. Contrib Mineral Petrol 171, 7. https://doi.org/10.1007/s00410-015-1212-x

Hesse, M., Grove, T.L., 2003. Absarokites from the western Mexican Volcanic Belt: constraints on mantle wedge conditions. Contributions to Mineralogy and Petrology 146, 10–27. https://doi.org/10.1007/s00410-003-0489-3

Hilley, G., 2022. SZ4D Implementation Plan. Stanford Digital Repository. https://doi.org/10.25740/HY589FC7561

Hirschmann, M.M., Ghiorso, M.S., Davis, F.A., Gordon, S.M., Mukherjee, S., Grove, T.L., Krawczynski, M., Medard, E., Till, C.B., 2008. Library of Experimental Phase Relations (LEPR): A database and Web portal for experimental magmatic phase equilibria data: LIBRARY OF EXPERIMENTAL PHASE RELATIONS. Geochem. Geophys. Geosyst. 9, n/a-n/a. https://doi.org/10.1029/2007GC001894

Hollyday, A.E., Leiter, S.H., Walowski, K.J., 2020. Pre-eruptive storage, evolution, and ascent timescales of a high-Mg basaltic andesite in the southern Cascade Arc. Contrib Mineral Petrol 175, 88. https://doi.org/10.1007/s00410-020-01730-z

Husen, A., Almeev, R.R., Holtz, F., 2016. The Effect of H2O and Pressure on Multiple Saturation and Liquid Lines of Descent in Basalt from the Shatsky Rise. Journal of Petrology 57, 309–344. https://doi.org/10.1093/petrology/egw008

Iacovino, K., Matthews, S., Wieser, P.E., Moore, G., Begue, F., 2021. VESIcal Part I: An open-source thermodynamic model engine for mixed volatile (H2O-CO2) solubility in silicate melt. Earth and Space Science. https://doi.org/10.1029/2020EA001584

Jeffery, A.J., Gertisser, R., Troll, V.R., Jolis, E.M., Dahren, B., Harris, C., Tindle, A.G., Preece, K., O'Driscoll, B., Humaida, H., Chadwick, J.P., 2013. The pre-eruptive magma plumbing system of the 2007–2008 dome-forming eruption of Kelut volcano, East Java, Indonesia. Contrib Mineral Petrol 166, 275–308. https://doi.org/10.1007/s00410-013-0875-4

Jorgenson, C., Higgins, O., Petrelli, M., Bégué, F., Caricchi, L., 2022. A Machine Learning-Based Approach to Clinopyroxene Thermobarometry: Model Optimization and Distribution for Use in Earth Sciences. JGR Solid Earth 127. https://doi.org/10.1029/2021JB022904

Kawamoto, T., 1996. Experimental constraints on differentiation and H2O abundance of calc-alkaline magmas. Earth and Planetary Science Letters 144, 577–589. https://doi.org/10.1016/S0012-821X(96)00182-3

Kelley, K.A., Cottrell, E., 2009. Water and the Oxidation State of Subduction Zone Magmas. Science 325, 605–607. https://doi.org/10.1126/science.1174156

Krawczynski, M.J., Grove, T.L., Behrens, H., 2012. Amphibole stability in primitive arc magmas: effects of temperature, H2O content, and oxygen fugacity. Contrib Mineral Petrol 164, 317–339. https://doi.org/10.1007/s00410-012-0740-x

Kress, V.C., Carmichael, I.S.E., 1988. Stoichiometry of the iron oxidation reaction in silicate melts. American Mineralogist.

Lai, Z., Zhao, G., Han, Z., Huang, B., Li, M., Tian, L., Liu, B., Bu, X., 2018. The magma plumbing system in the Mariana Trough back-arc basin at 18° N. Journal of Marine Systems 180, 132–139. https://doi.org/10.1016/j.jmarsys.2016.11.008

Lindsley, D.H., 1983. Pyroxene thermometry. American Mineralogist 68 (5–6), 477–493.

Lormand, C., Zellmer, G.F., Kilgour, G.N., Németh, K., Palmer, A.S., Sakamoto, N., Yurimoto, H., Kuritani, T., Iizuka, Y., Moebis, A., 2021. Slow Ascent of Unusually Hot Intermediate Magmas Triggering Strombolian to Sub-Plinian Eruptions. Journal of Petrology 61, egaa077. https://doi.org/10.1093/petrology/egaa077

Mandler, B.E., Donnelly-Nolan, J.M., Grove, T.L., 2014. Straddling the tholeiitic/calc-alkaline transition: the effects of modest amounts of water on magmatic differentiation at Newberry Volcano, Oregon. Contrib Mineral Petrol 168, 1066. https://doi.org/10.1007/s00410-014-1066-7

Martel, C., Pichavant, M., Holtz, F., Scaillet, B., Bourdier, J.-L., Traineau, H., 1999. Effects of f_{O2} and H_2O on andesite phase relations between 2 and 4 kbar. J. Geophys. Res. 104, 29453–29470. https://doi.org/10.1029/1999JB900191

Marxer, F., Ulmer, P., Müntener, O., 2022. Polybaric fractional crystallisation of arc magmas: an experimental study simulating trans-crustal magmatic systems. Contrib Mineral Petrol 177, 3. https://doi.org/10.1007/s00410-021-01856-8

Masotta, M., Keppler, H., Chaudhari, A., 2016. Fluid-melt partitioning of sulfur in differentiated arc magmas and the sulfur yield of explosive volcanic eruptions. Geochimica et Cosmochimica Acta 176, 26–43. https://doi.org/10.1016/j.gca.2015.12.014

McCanta, M.C., Dyar, M.D., Steven, C., Gunter, M., Lanzirotti, A., 2018. IN SITU MEASUREMENTS OF FE3+ IN PYROXENE USING X-RAY ABSORPTION SPECTROSCOPY: USING AN ORIENTED CRYSTAL CALIBRATION TO REFINE GEOTHERMOBAROMETRIC 2.

Melekhova, E., Blundy, J., Robertson, R., Humphreys, M.C.S., 2015. Experimental Evidence for Polybaric Differentiation of Primitive Arc Basalt beneath St. Vincent, Lesser Antilles. Journal of Petrology 56, 161–192. https://doi.org/10.1093/petrology/egu074

Mercer, C.N., Johnston, A.D., 2008. Experimental studies of the P–T–H2O near-liquidus phase relations of basaltic andesite from North Sister Volcano, High Oregon Cascades: constraints on lower-crustal mineral assemblages. Contrib Mineral Petrol 155, 571–592. https://doi.org/10.1007/s00410-007-0259-8

Mollo, S., Putirka, K., Misiti, V., Soligo, M., Scarlato, P., 2013. A new test for equilibrium based on clinopyroxene–melt pairs: Clues on the solidification temperatures of Etnean alkaline melts at post-eruptive conditions. Chemical Geology 352, 92–100. https://doi.org/10.1016/j.chemgeo.2013.05.026

Moore, G., Carmichael, I.S.E., 1998. The hydrous phase equilibria (to 3 kbar) of an andesite and basaltic andesite from western Mexico: constraints on water content and conditions of phenocryst growth. Contributions to Mineralogy and Petrology 130, 304–319. https://doi.org/10.1007/s004100050367

Moussallam, Y., Médard, E., Georgeais, G., Rose-Koga, E.F., Koga, K.T., Pelletier, B., Bani, P., Shreve, T.L., Grandin, R., Boichu, M., Tari, D., Peters, N., 2021. How to turn off a lava lake? A petrological investigation of the 2018 intra-caldera and submarine eruptions of Ambrym volcano. Bull Volcanol 83, 36. https://doi.org/10.1007/s00445-021-01455-2

Moussallam, Y., Rose-Koga, E.F., Koga, K.T., Médard, E., Bani, P., Devidal, J.-L., Tari, D., 2019. Fast ascent rate during the 2017–2018 Plinian eruption of Ambae (Aoba) volcano: a petrological investigation. Contrib Mineral Petrol 174, 90. https://doi.org/10.1007/s00410-019-1625-z

Nakatani, T., Kudo, T., Suzuki, T., 2022. Experimental Constraints on Magma Storage Conditions of Two Caldera-Forming Eruptions at Towada Volcano, Japan. JGR Solid Earth 127. https://doi.org/10.1029/2021JB023665

Namur, O., Montalbano, S., Bolle, O., Vander Auwera, J., 2020. Petrology of the April 2015 Eruption of Calbuco Volcano, Southern Chile. Journal of Petrology 61, egaa084. https://doi.org/10.1093/petrology/egaa084

Nandedkar, R.H., Ulmer, P., Müntener, O., 2014. Fractional crystallization of primitive, hydrous arc magmas: an experimental study at 0.7 GPa. Contrib Mineral Petrol 167, 1015. https://doi.org/10.1007/s00410-014-1015-5

Neave, D.A., Bali, E., Guðfinnsson, G.H., Halldórsson, S.A., Kahl, M., Schmidt, A.-S., Holtz, F., 2019. Clinopyroxene–Liquid Equilibria and Geothermobarometry in Natural and Experimental Tholeiites: the 2014–2015 Holuhraun Eruption, Iceland. Journal of Petrology 60, 1653–1680. https://doi.org/10.1093/petrology/egz042

Neave, D.A., Putirka, K.D., 2017. A new clinopyroxene-liquid barometer, and implications for magma storage pressures under Icelandic rift zones. American Mineralogist 102, 777–794. https://doi.org/10.2138/am-2017-5968

Nimis, P., 1999. Clinopyroxene geobarometry of magmatic rocks. Part 2. Structural geobarometers for basic to acid, tholeiitic and mildly alkaline magmatic systems. Contrib Mineral Petrol 135, 62–74. https://doi.org/10.1007/s004100050498

Parat, F., Streck, M., Holtz, F., Almeev, R.R., 2014. Experimental study into the petrogenesis of crystal-rich basaltic to andesitic magmas at Arenal volcano. Contributions to Mineralogy and Petrology.

Parman, S.W., Grove, T.L., Kelley, K.A., Plank, T., 2011. Along-Arc Variations in the Pre-Eruptive H2O Contents of Mariana Arc Magmas Inferred from Fractionation Paths. Journal of Petrology 52, 257–278. https://doi.org/10.1093/petrology/egq079

Petrelli, M., Caricchi, L., Perugini, D., 2020. Machine Learning Thermo-Barometry: Application to Clinopyroxene-Bearing Magmas. J. Geophys. Res. Solid Earth 125. https://doi.org/10.1029/2020JB020130

Pichavant, M., Macdonald, R., 2007. Crystallization of primitive basaltic magmas at crustal pressures and genesis of the calc-alkaline igneous suite: experimental evidence from St Vincent, Lesser Antilles arc. Contrib Mineral Petrol 154, 535–558. https://doi.org/10.1007/s00410-007-0208-6

Plank, T., Kelley, K.A., Zimmer, M.M., Hauri, E.H., Wallace, P.J., 2013. Why do mafic arc magmas contain ~4wt% water on average? Earth and Planetary Science Letters 364, 168–179. https://doi.org/10.1016/j.epsl.2012.11.044

Preece, K., Gertisser, R., Barclay, J., Berlo, K., Herd, R.A., 2014. Pre- and syn-eruptive degassing and crystallisation processes of the 2010 and 2006 eruptions of Merapi volcano, Indonesia. Contrib Mineral Petrol 168, 1061. https://doi.org/10.1007/s00410-014-1061-z

Profeta, L., Ducea, M.N., Chapman, J.B., Paterson, S.R., Gonzales, S.M.H., Kirsch, M., Petrescu, L., DeCelles, P.G., 2016. Quantifying crustal thickness over time in magmatic arcs. Sci Rep 5, 17786. https://doi.org/10.1038/srep17786

Putirka, K., 1999. Clinopyroxene + liquid equilibria to 100 kbar and 2450 K. Contributions to Mineralogy and Petrology 135, 151–163. https://doi.org/10.1007/s004100050503

Putirka, K.D., 2008a. Thermometers and Barometers for Volcanic Systems. Reviews in Mineralogy and Geochemistry 69, 61–120. https://doi.org/10.2138/rmg.2008.69.3

Putirka, K.D., 2008b. Thermometers and Barometers for Volcanic Systems. Reviews in Mineralogy and Geochemistry 69, 61–120. https://doi.org/10.2138/rmg.2008.69.3

Putirka, K.D., Mikaelian, H., Ryerson, F., Shaw, H., 2003. New clinopyroxene-liquid thermobarometers for mafic, evolved, and volatile-bearing lava compositions, with applications to lavas from Tibet and the Snake River Plain, Idaho. American Mineralogist 88, 1542–1554. https://doi.org/10.2138/am-2003-1017

Rader, E.L., Larsen, J.F., 2013. Experimental phase relations of a low MgO Aleutian basaltic andesite at XH2O = 0.7–1. Contrib Mineral Petrol 166, 1593–1611. https://doi.org/10.1007/s00410-013-0944-8

Riker, J.M., Blundy, J.D., Rust, A.C., Botcharnikov, R.E., Humphreys, M.C.S., 2015. Experimental phase equilibria of a Mount St. Helens rhyodacite: a framework for interpreting crystallization paths in degassing silicic magmas. Contrib Mineral Petrol 170, 6. https://doi.org/10.1007/s00410-015-1160-5

Romero, J.E., Morgado, E., Pisello, A., Boschetty, F., Petrelli, M., Cáceres, F., Alam, M.A., Polacci, M., Palma, J.L., Arzilli, F., Vera, F., Gutiérrez, R., Morgavi, D., 2022. Pre-eruptive Conditions of the 3 March 2015 Lava Fountain of Villarrica Volcano (Southern Andes). Bull Volcanol 85, 2. https://doi.org/10.1007/s00445-022-01621-0

Rudra, A., 2021. FERRIC IRON PARTITIONING BETWEEN PYROXENE AND MELT: EXPERIMENTS, MICROBEAM ANALYSIS, AND CONSEQUENCES FOR MANTLE REDOX. PhD thesis, University of Minnesota.

Ruth, D.C.S., Costa, F., 2021. A petrological and conceptual model of Mayon volcano (Philippines) as an example of an open-vent volcano. Bull Volcanol 83, 62. https://doi.org/10.1007/s00445-021-01486-9

Rutherford, M.J., Sigurdsson, H., Carey, S., Davis, A., 1985. The May 18, 1980, eruption of Mount St. Helens: 1. Melt composition and experimental phase equilibria. J. Geophys. Res. 90, 2929. https://doi.org/10.1029/JB090iB04p02929

Sas, M., DeBari, S., Clynne, M., Rusk, B., 2017. Using mineral geochemistry to decipher slab, mantle, and crustal input in the generation of high-Mg andesites and basaltic andesites from the northern Cascade Arc. msam. https://doi.org/10.2138/am-2017-5756

Scruggs, M.A., Putirka, K.D., 2018. Eruption triggering by partial crystallization of mafic enclaves at Chaos Crags, Lassen Volcanic Center, California. American Mineralogist 103, 1575–1590. https://doi.org/10.2138/am-2018-6058

Sheehan, F., Barclay, J., 2016. Staged storage and magma convection at Ambrym volcano, Vanuatu. Journal of Volcanology and Geothermal Research 322, 144–157. https://doi.org/10.1016/j.jvolgeores.2016.02.024

Sisson, T.W., Ratajeski, K., Hankins, W.B., Glazner, A.F., 2005. Voluminous granitic magmas from common basaltic sources. Contrib Mineral Petrol 148, 635–661. https://doi.org/10.1007/s00410-004-0632-9

Sobolev, V.N., McCammon, C.A., Taylor, L.A., Snyder, G.A., Sobolev, N.V., 1999. Precise Moessbauer milliprobe determination of ferric iron in rock-forming minerals and limitations of electron microprobe analysis. American Mineralogist 84, 78–85. https://doi.org/10.2138/am-1999-1-208

Solaro, C., Martel, C., Champallier, R., Boudon, G., Balcone-Boissard, H., Pichavant, M., 2019. Petrological and experimental constraints on magma storage for large pumiceous eruptions in Dominica island (Lesser Antilles). Bull Volcanol 81, 55. https://doi.org/10.1007/s00445-019-1313-x

Tommasini, S., Bindi, L., Savia, L., Mangler, M.F., Orlando, A., Petrone, C.M., 2022. Critical assessment of pressure estimates in volcanic plumbing systems: The case study of Popocatépetl volcano, Mexico. Lithos 408–409, 106540. https://doi.org/10.1016/j.lithos.2021.106540

Ulmer, P., Kaegi, R., Müntener, O., 2018. Experimentally Derived Intermediate to Silica-rich Arc Magmas by Fractional and Equilibrium Crystallization at 1·0 GPa: an Evaluation of Phase Relationships, Compositions, Liquid Lines of Descent and Oxygen Fugacity. Journal of Petrology 59, 11–58. https://doi.org/10.1093/petrology/egy017

Wang, X., Hou, T., Wang, M., Zhang, C., Zhang, Z., Pan, R., Marxer, F., Zhang, H., 2021. A new clinopyroxene thermobarometer for mafic to intermediate magmatic systems. Eur. J. Mineral. 33, 621–637. https://doi.org/10.5194/ejm-33-621-2021

Waters, L.E., Cottrell, E., Coombs, M.L., Kelley, K.A., 2021. Generation of Calc-Alkaline Magmas during Crystallization at High Oxygen Fugacity: An Experimental and Petrologic Study of Tephras from Buldir Volcano, Western Aleutian Arc, Alaska, USA. Journal of Petrology 62, egaa104. https://doi.org/10.1093/petrology/egaa104

Wieser, P., Kent, A., Till, C., Donovan, J., Neave, D., Blatter, D., Mike Krawczynski, M., 2022a. Barometers behaving badly: Assessing the influence of analytical and experimental uncertainty on clinopyroxene thermobarometry calculations at crustal conditions (preprint). Earth Sciences. https://doi.org/10.31223/X5JT0N

Wieser, P., Petrelli, M., Lubbers, J., Wieser, E., Ozaydin, S., Kent, A., Till, C., 2022b. Thermobar: An open-source Python3 tool for thermobarometry and hygrometry. Volcanica 5, 349–384. https://doi.org/10.30909/vol.05.02.349384

Wieser, P.E., Iacovino, K., Matthews, S., Moore, G., Allison, C.M., 2022c. VESIcal: 2. A Critical Approach to Volatile Solubility Modeling Using an Open-Source Python3 Engine. Earth and Space Science 9. https://doi.org/10.1029/2021EA001932

Wood, B.J., Blundy, J., 1997. predictive model for rare earth element partitioning between clinopyroxene and anhydrous silicate melt. Contributions to Mineralogy and Petrology.

Table 1– Compilation of Cpx-based thermobarometers used in studies of arc magmas. In many studies, we deduced the exact equations used through email correspondence with the authors (many papers simply stated Putirka, 2008 in the text).

Clinopyroxene-Liquid barometry	
P = Putirka (2008) eq31, T = Putirka (2008) eq33	**P = Neave & Putirka (2017), T = Putirka (2008) eq33**
• Mt Baker and Glacier Peak, Cascades - *Sas et al. (2017)* • Whangaeuhu Gorge, New Zealand **-** *Auer et al. (2013)*	• Ebeko Volcano, Kurile arc - *Belousov et al. (2021)* • Lassen Peak, Cascades - *Hollyday et al. (2020)* • Lassen Peak, Cascades - *Scruggs and Putirka, (2018)* • Taupo Volcanic Zone - *Lormand et al. (2021)* • Calbuco Volcano - *Namur et al. (2020)*
P = Putirka (2008) eq30, T = Putirka (2008) eq33	**P = Putirka (2003), T = Putirka (2003)**
• Agung and Batur, Indonesia - *Geiger et al. (2018)* • Ambae, Vanuatu - *Moussallam et al. (2019)* • Ambrym, Vanuatu - *Moussallam et al. (2021)* • Ambrym, Vanuatu - *Sheehan and Barclay (2016)* • Villarrica, Chile – *Romero et al. (2022)*	• Agung and Batur, Indonesia - *Geiger et al. (2018)* • Ambrym, Vanuatu - *Sheehan and Barclay (2016)* • Soufrière Hills, Monseratt - *Cassidy et al. (2015)* • Krakatau, Indonesia - *Dahren et al. (2012)* • Tofua Volcano, Tonga - *Caulfield et al. (2012)*
P = Putirka (2008) eq32c, T = …	
T = Putirka (1996) eqT2 (spreadsheet default): • Mayon Volcano, Phillipines - *Ruth and Costa (2021)* **Thermometer not stated in paper:** • Miravalles-Guayabo Caldera, Costa Rica - *Cigolini et al. (2018)* • Mt Baker and Glacier Peak, Cascades - *Sas et al. (2017)*	**T = Putirka (2008) eq33:** • Chiltepe, Nicaragua - *Freundt and Kutterolf (2019)* **T = Putirka (2003)** • Agung and Batur, Indonesia - *Geiger et al. (2018)* • Merapi, Indonesia - *Preece et al. (2014)* • Krakatau, Indonesia - *Dahren et al. (2012)*
Cpx-only Barometry	
P = Putirka (2003) eq32b, T = …	**P = Putirka (2008) eq32a, T=…**
Thermometer not stated in paper: • Agung and Batur, Indonesia - *Geiger et al. (2018)* • Merapi Volcano, Indonesia - *Deegan et al. (2016)* • Ambae, Vanuatu - *Moussallam et al. (2019)* • Merapi, Indonesia - *Preece et al. (2014)* **T = Putirka (2008) eq32d:** • Kelut Volcano, Indonesia - *Jeffery et al. (2013)* **T = Putirka (2008) eq33:** • Chiltepe Volcanic Complex, Nicaragua - *Freundt and Kutterolf, (2019)* **T from P1996:** • Etna, Italy - *Ubide and Kamber, (2018)*	**Thermometer not stated in paper:** • Taupo Volcanic Zone - *Beier et al. (2017)* **T from P2003:** • Volcan Melimoyu, Andes. *Geoffroy et al. (2018)* **T from P2008 eq32d:** • Ambrym, Vanuatu - *Sheehan and Barclay (2016)* • Ambrym, Vanuatu - *Moussallam et al. (2021)* **T from P2008 eq33:** • Mariana trough back-arc basin - *Lai et al. (2018)* • Okinawa Trough - *Chen et al. (2021)*

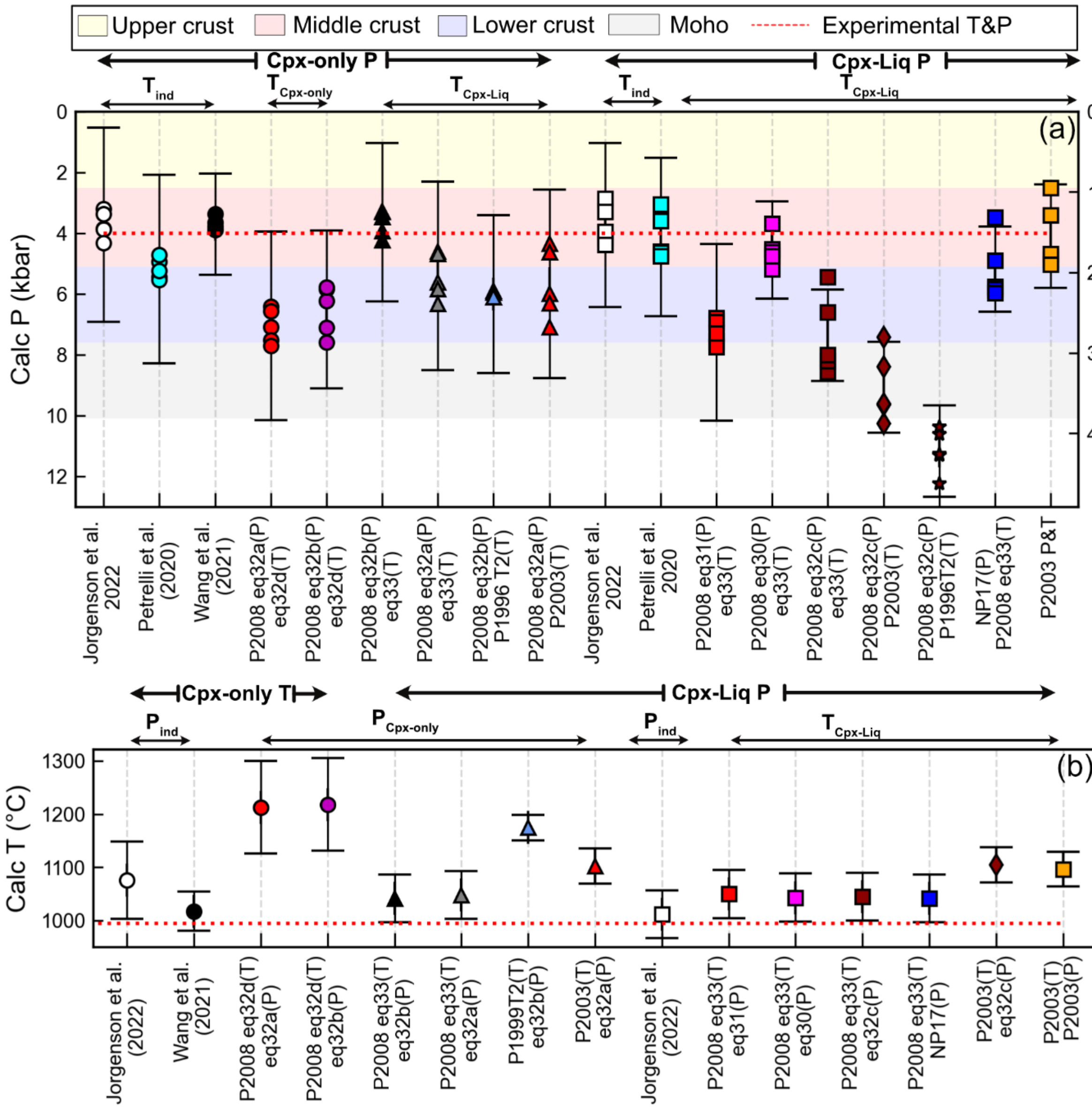

Figure 1 – Comparison of calculated P and T using the various combinations of thermometers and barometers summarized in Table 1. a) Barometry calculations performed for the five experiments of Blatter et al. (2013) performed at 4 kbar (#2381, 2390, 2380, 2391, 2389). b) Temperatures calculated for experiment #2358 conducted at 995˚C, 5.5 wt% H_2O, 9 kbar from Blatter et al. (2013). Error bars are plotted at the average calculated P, and calculated T, showing the quoted RMSE from each equation. Crustal pressure bins are the same as the boundaries used in later figures, based on the distribution of pressures in the ArcPL dataset, and the crustal thickness dataset of Profeta et al. (2016). See Supporting Fig. 1 for the same comparison for 7 kbar experiments.

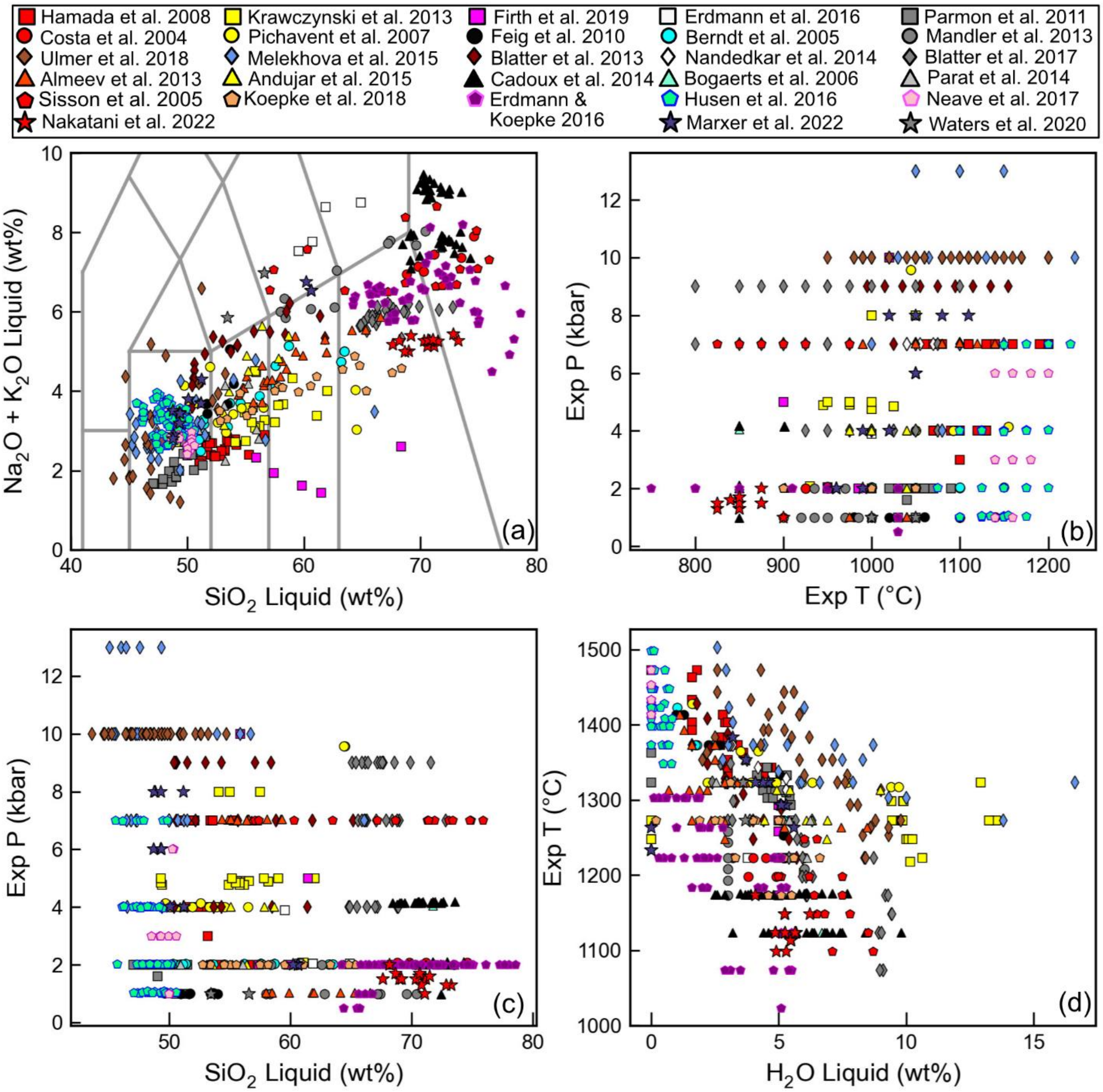

Figure 2 – Compositional and P-T spread for the ArcPL dataset before the application of filters for Cpx-Liq equilibrium, cation sums, number of analyses and melt H_2O contents.

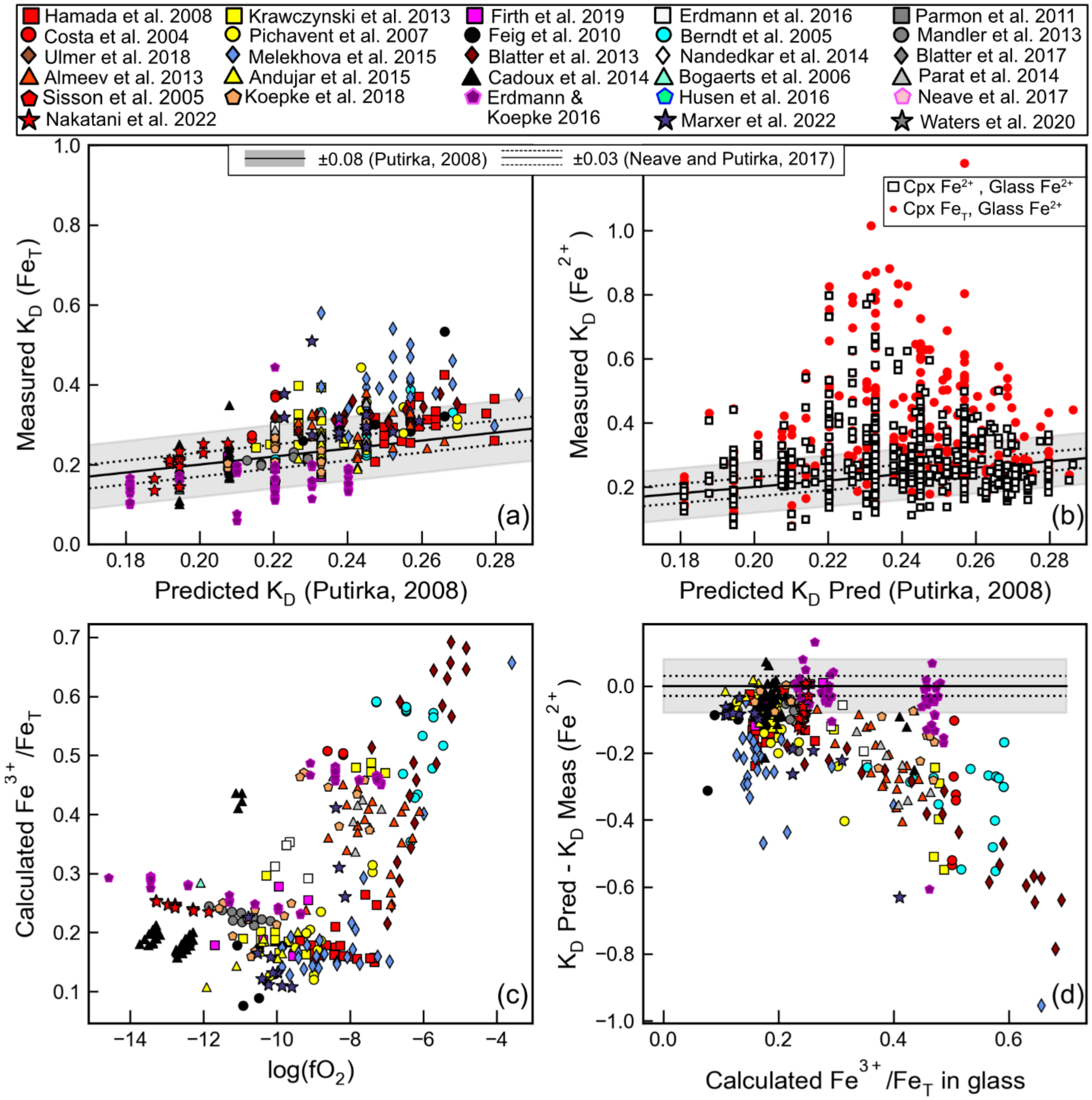

Figure 3 - Assessment of Fe-Mg partitioning between Cpx and Liq (K_D) in the ArcPL dataset. a-b) Predicted values calculated using Putirka (2008) eq35. vs. measured values. In a), Fe_T is used in Cpx and Glass to calculate the measured value. In b) the red dots show calculations using Fe^2 in the liquid calculated calculated using Kress and Carmichael (1988) from the quoted experimental fo_2 or redox buffer (see part c), and Fe_T in the Cpx. Black squares show Fe^{2+} in the liquid and Fe^{2+} in the Cpx calculated using Lindsley and Andersen (1983). d) The discrepancy between calculated and predicted K_D values using Fe^{2+} in the liquid and Fe_T in the Cpx increases with increasing proportion of $Fe^{3.}$ Dashed lines show the ±0.03 value used for equilibrium tests by Neave et al. (2019), while the grey field shows the ±0.08 value suggested by Putirka (2008).

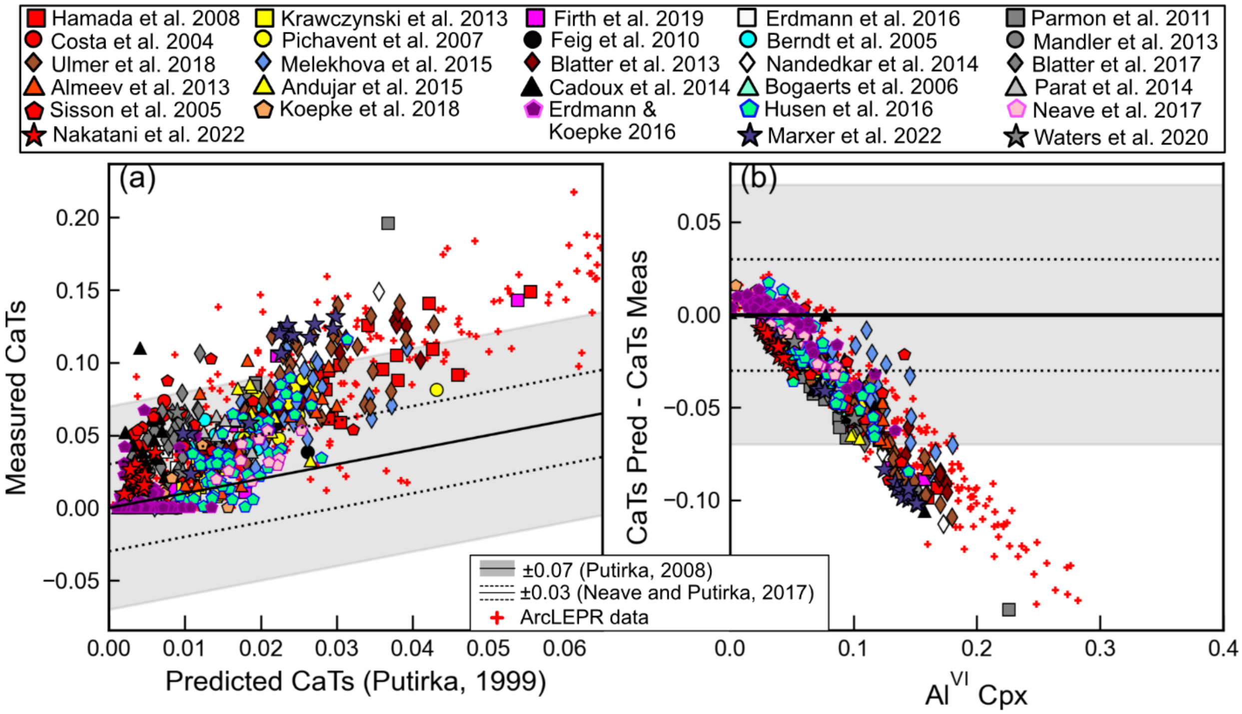

Figure 4 – a) Comparison of predicted and measured values of CaTs. The grey colored box shows the ±0.07 error window suggested by Putirka, (1999), and the dashed lines show the ±0.03 value used by Neave et al. (2019) to filter natural Cpx-Liq pairs. b) There is a strong correlation between the discrepancy and the Al^{VI} component of Cpx.

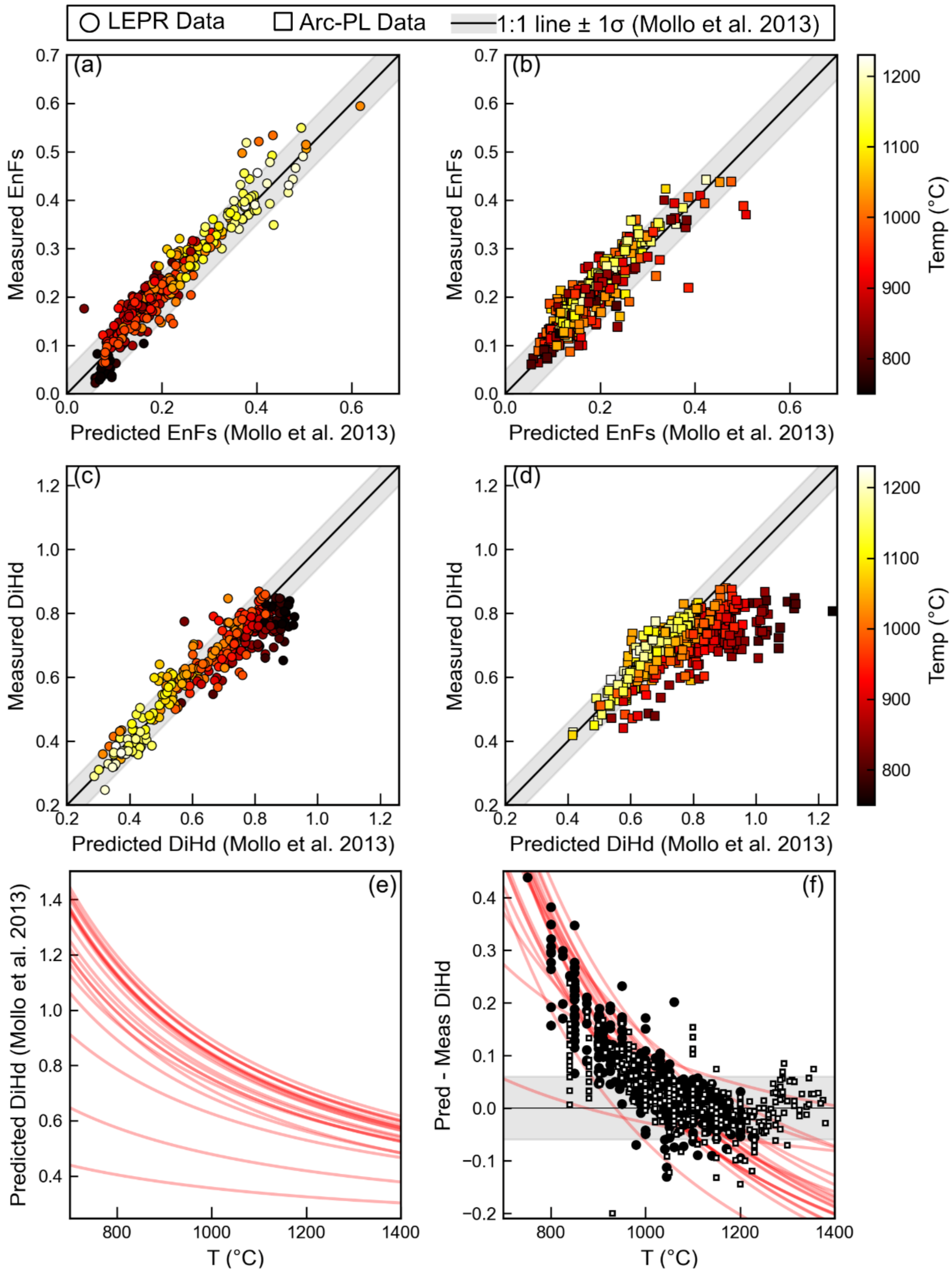

Figure 5 - Comparison of measured values of EnFs and DiHd with those predicted from the expression of Mollo et al. (2013). In a), the grey bar shows ±0.05, while in b), the grey bar shows ±0.06 (both cutoffs from Mollo et al. 2013). Symbols are coloured based on the experimental temperature. e) Predicted values of DiHd as a function of temperature using the expression of Mollo et al. (2013) for 20 randomly-selected Cpx-Liq pairs. e) The discrepancy between predicted and measured DiHd contents for these 20 Cpxs (red lines), with experimental data from Arc-PL (black dots) and LEPR (white squares) overlain.

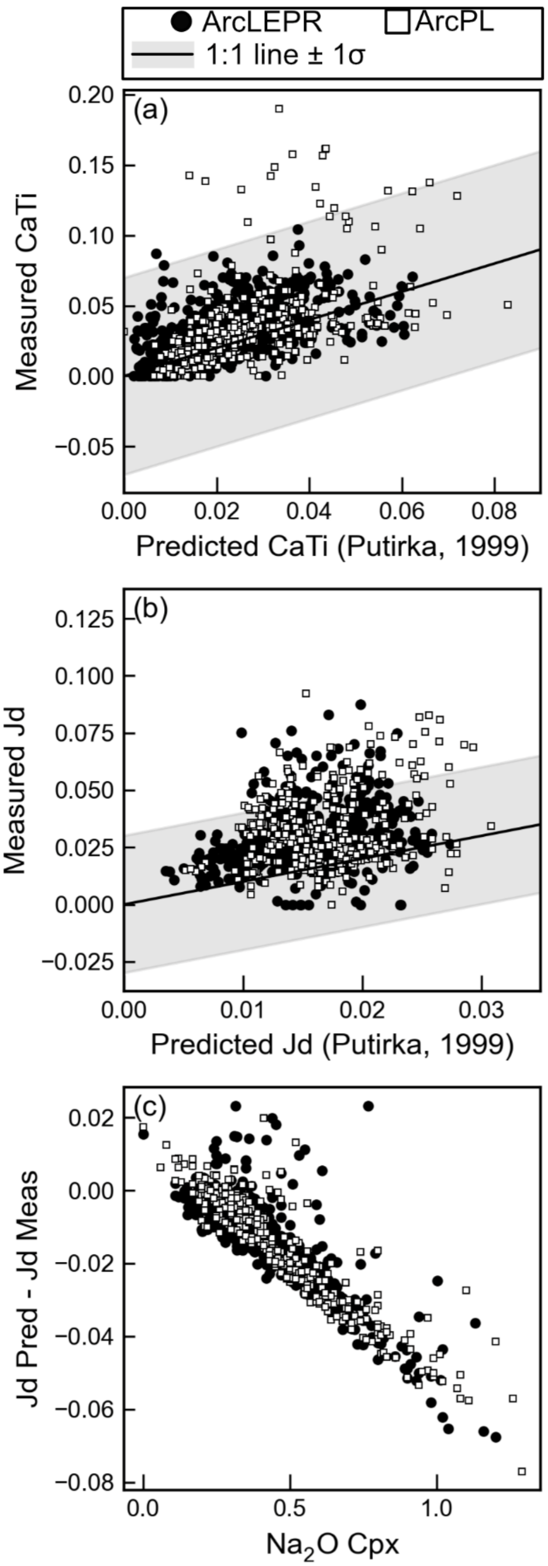

Figure 6 - The discrepancy between calculated and measured a) CaTi and b) Jd components. The discrepancy increases as a function of Na_2O content of the Cpx.

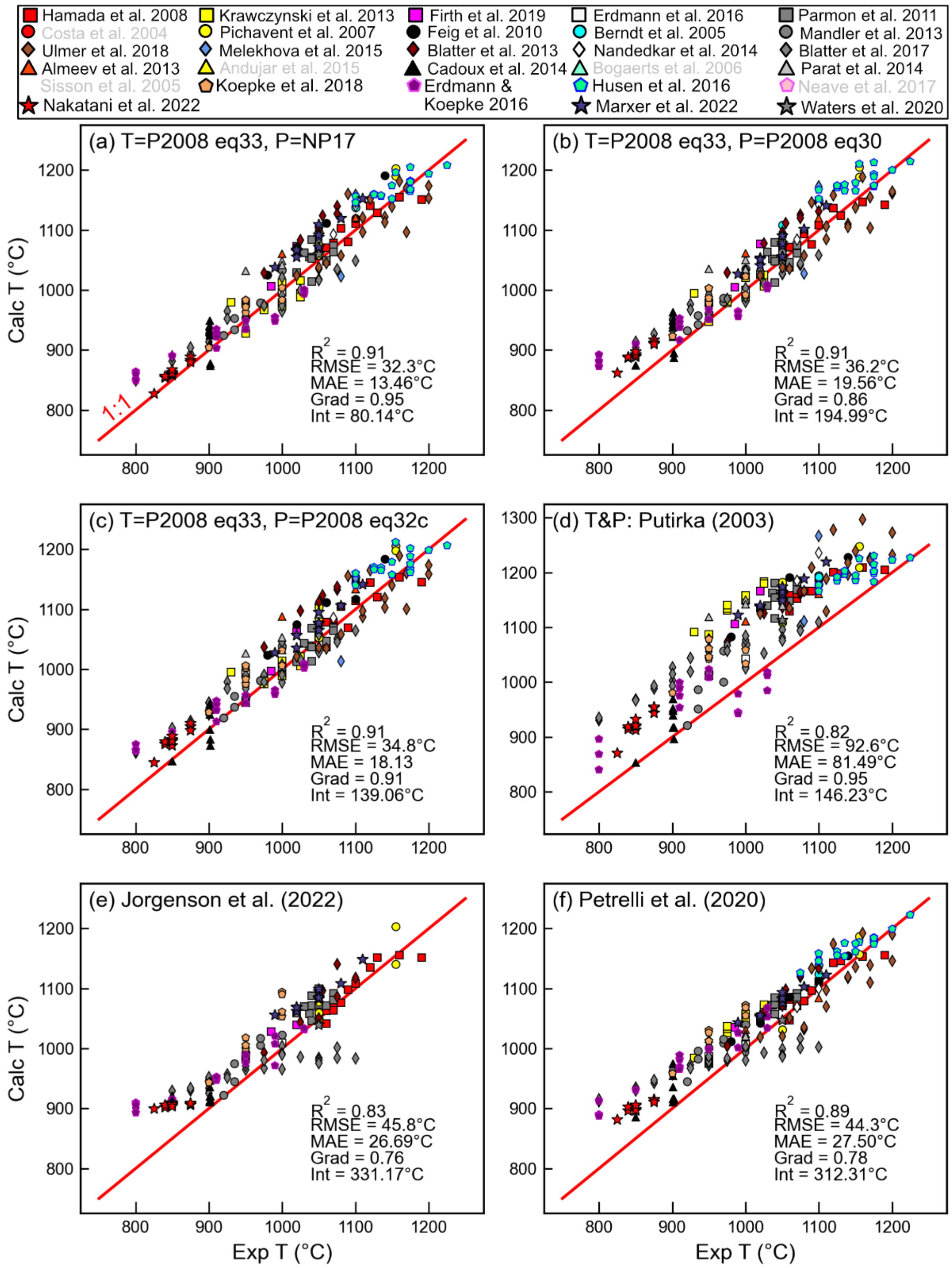

Fig. 7 – Evaluation of various Cpx-Liq thermometers (iterating P and T) for the filtered ArcPL dataset. Experimental studies which failed equilibrium or quality filters are greyed out in the legend. The best thermometer appears to be Putirka (2008) eq 33 iterated with Neave and Putirka (2017), indicated by the gold trophy symbol. When testing the Jorgenson et al. (2022) expression, experiments in their calibration dataset are excluded, resulting in fewer symbols being shown on this panel than others. In the legend, studies where all experiments failed the equilibrium or quality filters are greyed out. A red 1:1 line is shown on each plot.

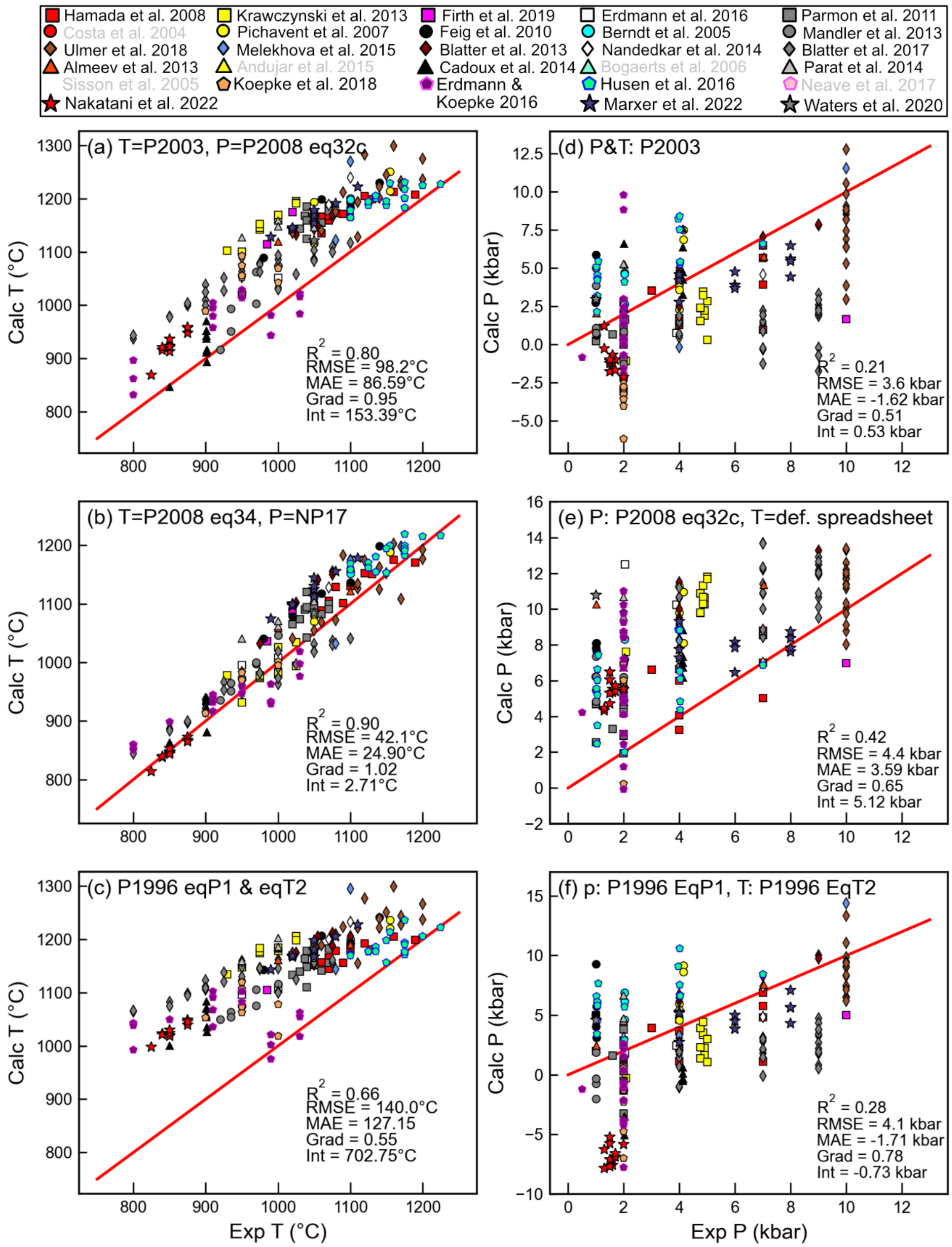

Fig. 8– Evaluation of various Cpx-Liq thermobarometers (iterating P and T) using experimental water contents for the filtered ArcPL dataset for and temperature (left columns, parts a-c) and pressure (right columns, parts d-f)

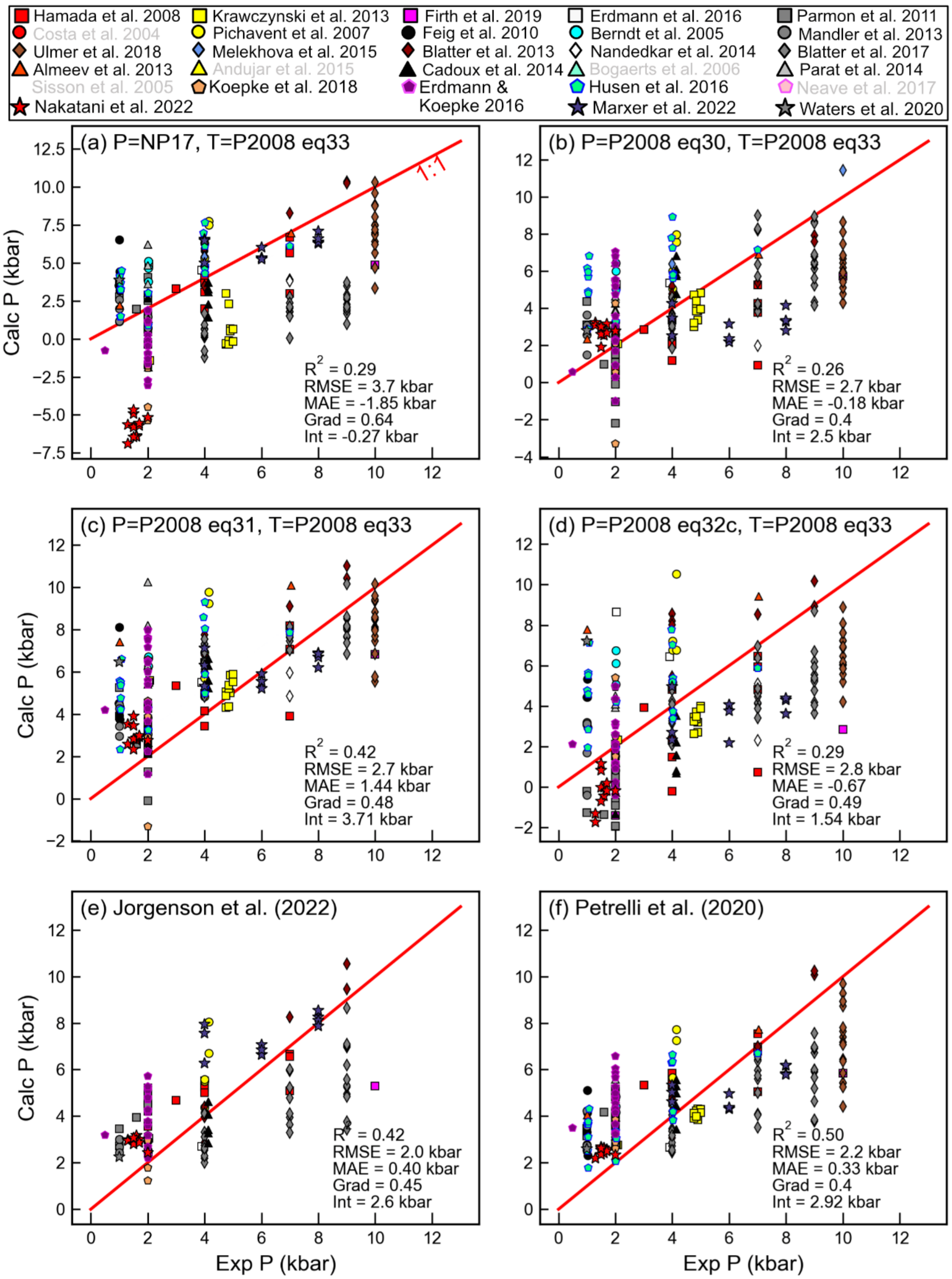

Fig 9 – Evaluation of Cpx-Liq pressures for the filtered ArcPL dataset.

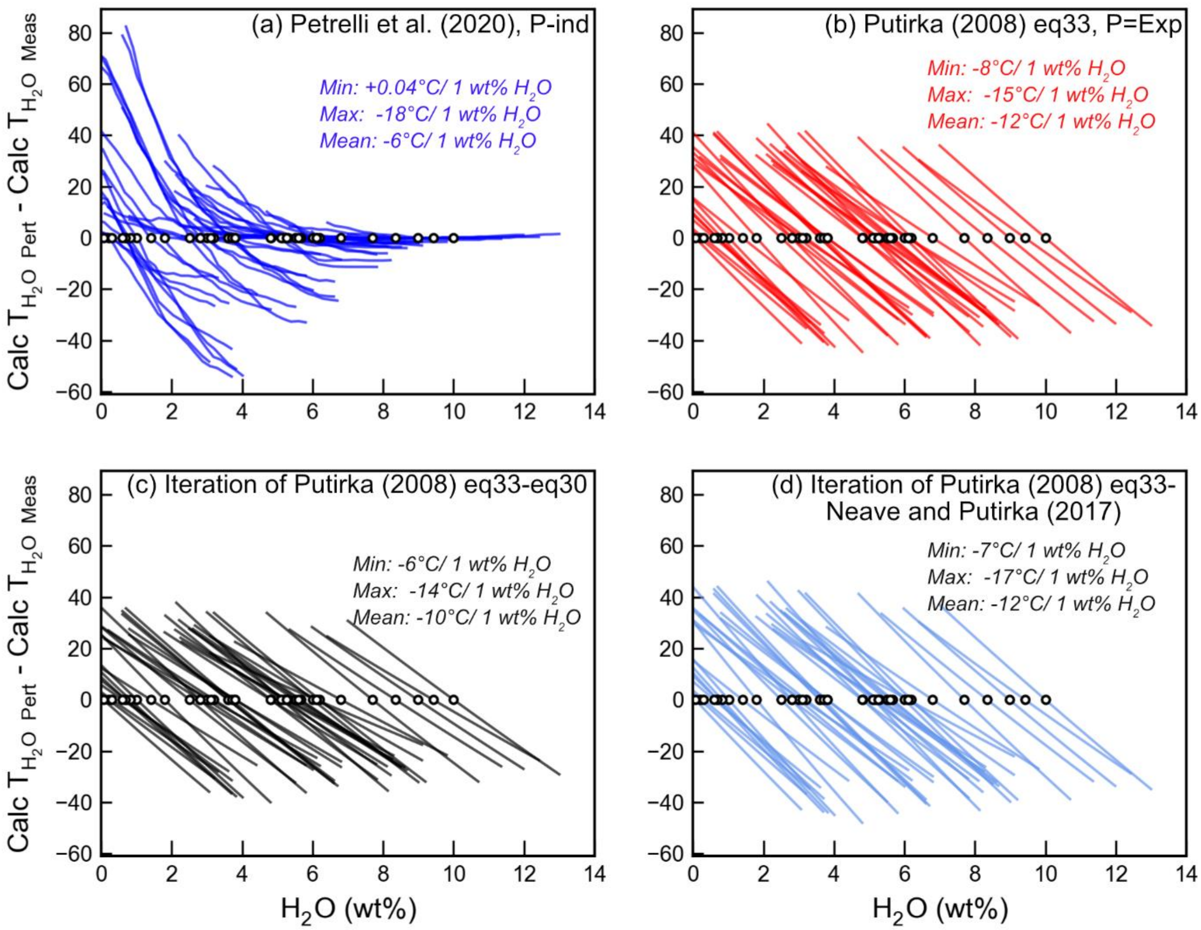

Figure 10 - Sensitivity of calculated temperature to melt H_2O content for 41 randomly selected Cpx-Liq pairs. For each Cpx-Liq pair, we add a linearly-spaced ranging from -3 to +3 to the experimental H_2O content, and calculations are performed for each discrete H_2O value (e.g. for H_2O=4 wt%, calculations are performed from 1-7 wt%). The calculated temperature for the measured H_2O content are subtracted from the calculation for the perturbed H_2O content. This change in temperature for each Cpx-Liq pair is displayed as a colored line, passing through the H_2O content of the experiment (where the T discrepancy is 0). We calculate the max and min change in temperature, and the mean change, for all 41 selected pairs.

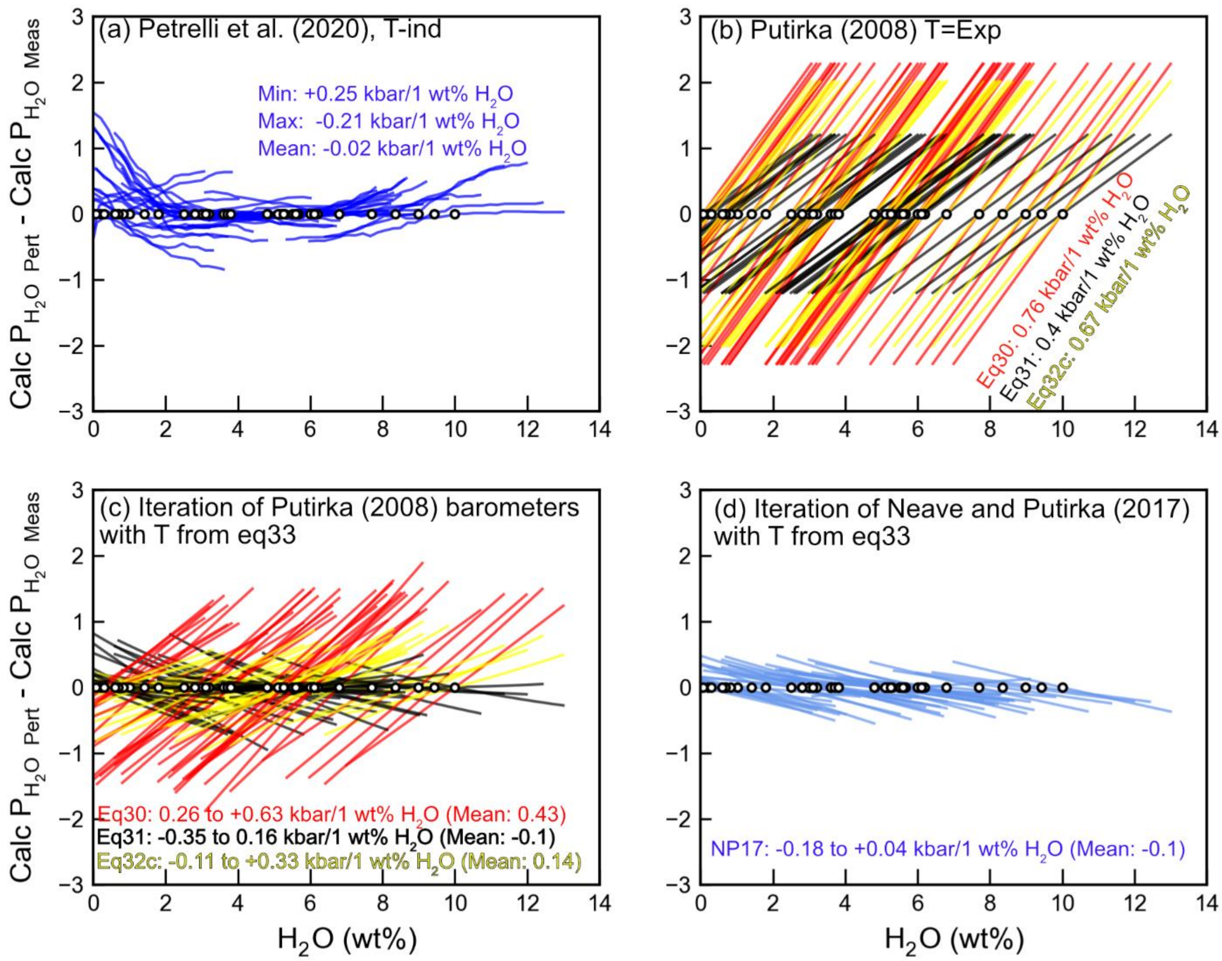

Figure 11 -Using the same method described in Fig. 10, we investigate the sensitivity of calculated pressure to H_2O.

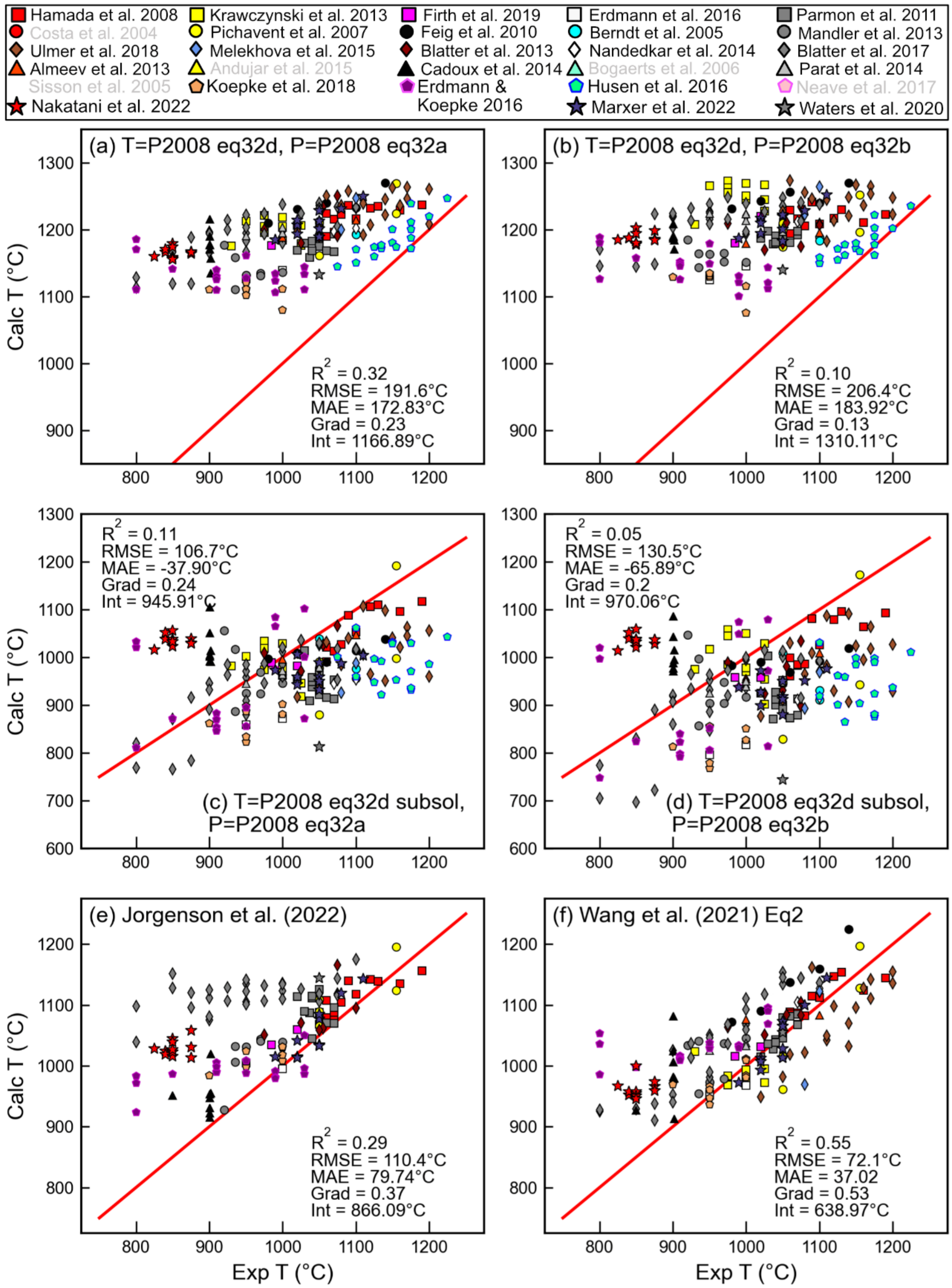

Figure 12 – Comparison of calculated and experimental temperatures for different Cpx-only thermobarometry combinations. For Jorgenson et al. (2022) and Wang et al. (2021), experiments in their calibration dataset are excluded.

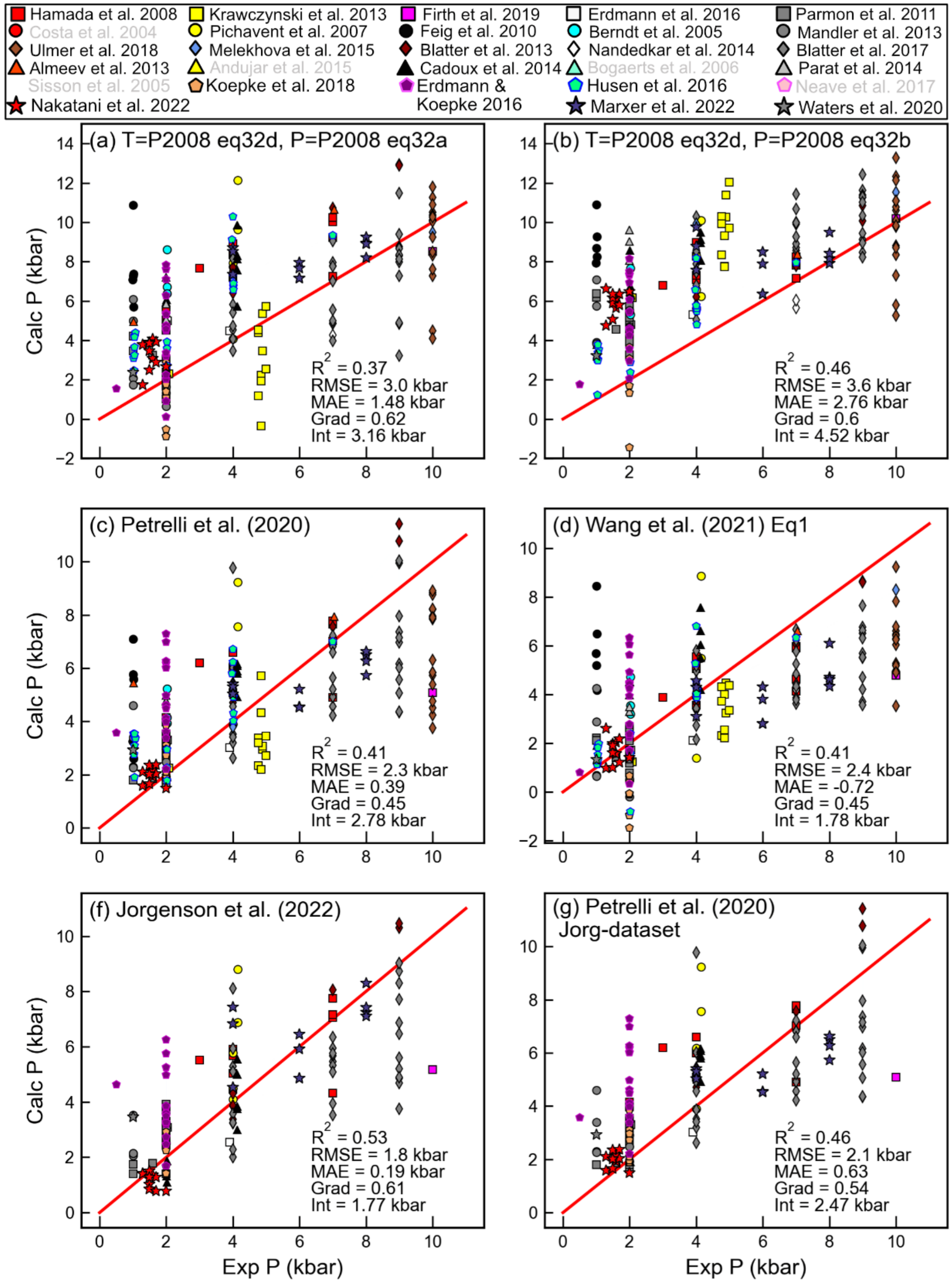

Figure 13 - Assessment of Cpx-only barometers. For Jorgenson et al. (2022) and Wang et al. (2021), experiments in their calibration dataset are excluded.

Figure 14

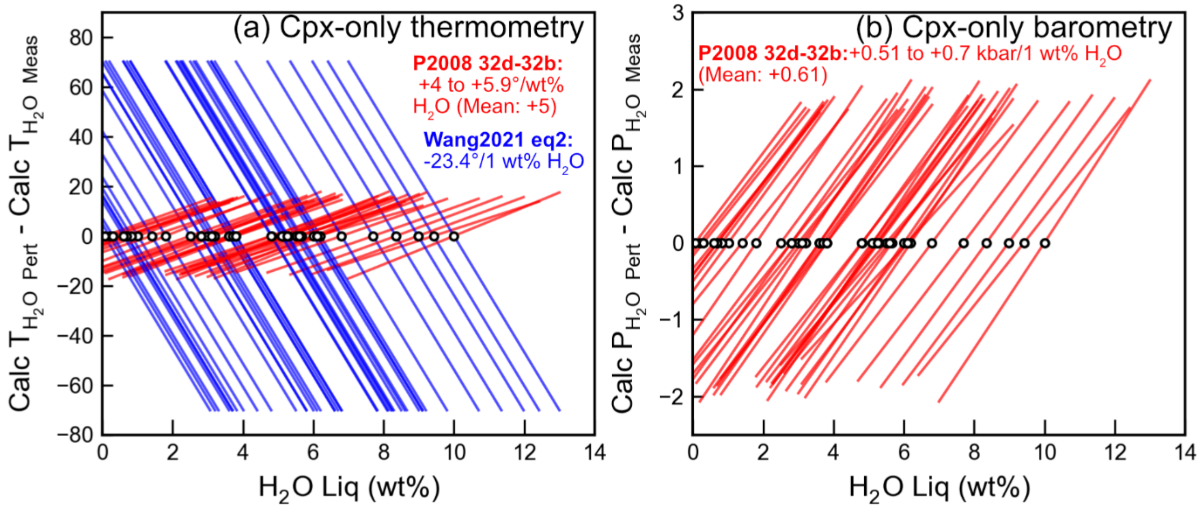

Figure 14 –As for Fig. 10, investigating the sensitivity of Cpx-only pressures and temperatures to H_2O content in the melt.

Figure 15

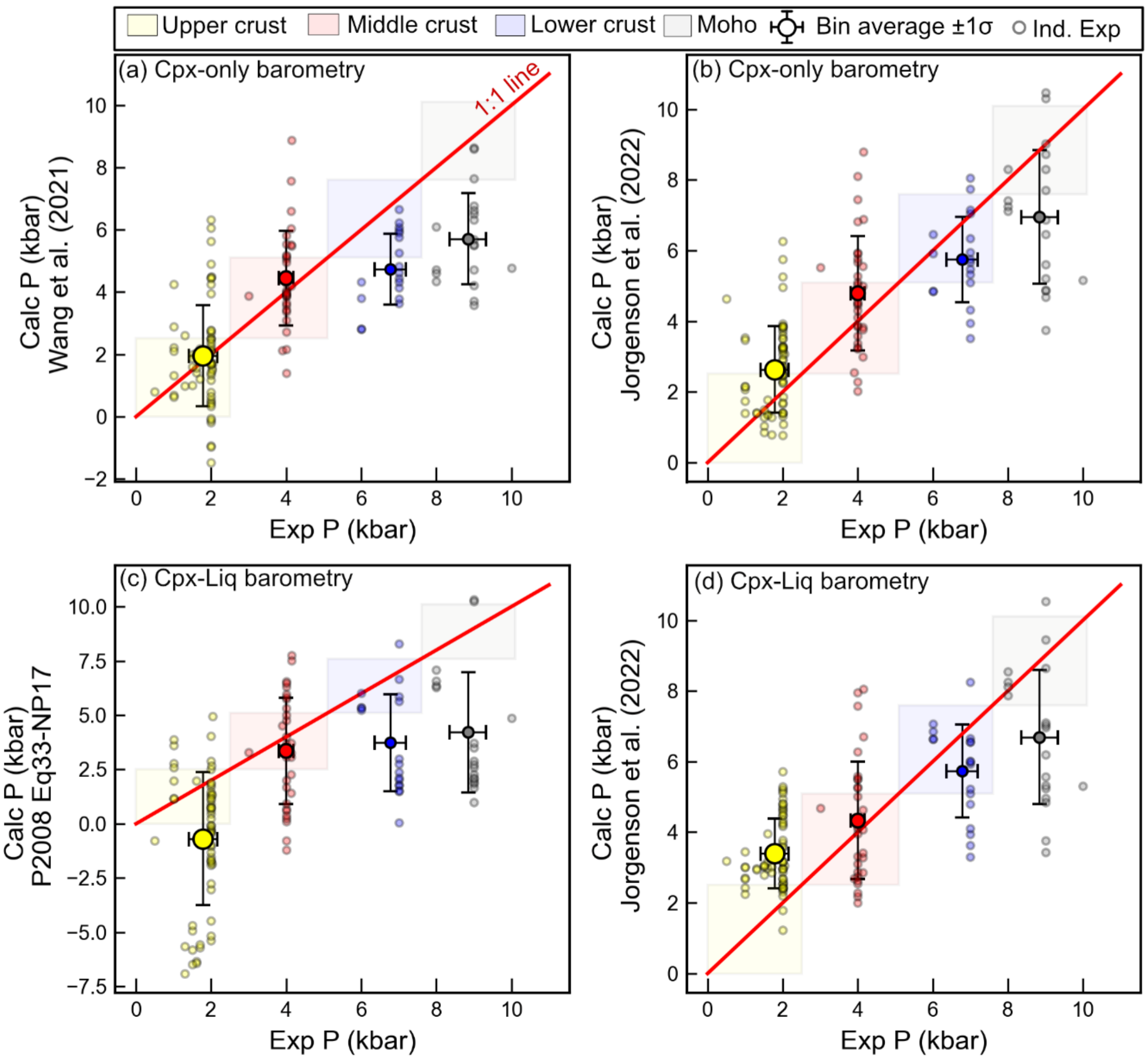

Fig 15 – Assessment of effect of averaging on Cpx-only (a-b) and Cpx-Liq barometry (c-d). The experimental pressures for all experiments lying within one of the 4 crustal bins (marked with transparent squares in pastel colors) are averaged, and compared to the mean of the calculated pressure for each expression. 1σ for these averages are shown with error bars, and the bin average is shown with a circle with the size corresponding to the number of averaged experiment (N=63 upper crust, N=32 middle crust, N=18 lower crust and N=19 Moho). The 1:1 line is also shown in red, and individual experiments are shown as semi-transparent symbols. Statistics for Tukey pairwise tests are shown in Supporting Fig. 13. Only experiments not present in the calibration datasets of Wang et al. (2021) and Jorgenson et al. (2022) are shown, for fair comparisons between barometers.

Supporting Information for "Barometers behaving badly II: A critical evaluation of Cpx-only and Cpx-Liq thermobarometry in variably-hydrous arc magmas"

Penny E. Wieser[1,2], Adam Kent[2], Christy Till[3]

1. **Corresponding author**: Penny_wieser@berkeley.edu. Department of Earth and Planetary Sciences, McCone Hall, UC Berkeley, 94720, USA
2. College of Earth, Ocean and Atmospheric Sciences, Oregon State University, 97331, USA
3. School of Earth and Space Exploration, Arizona State University, Tempe, AZ 85281, USA

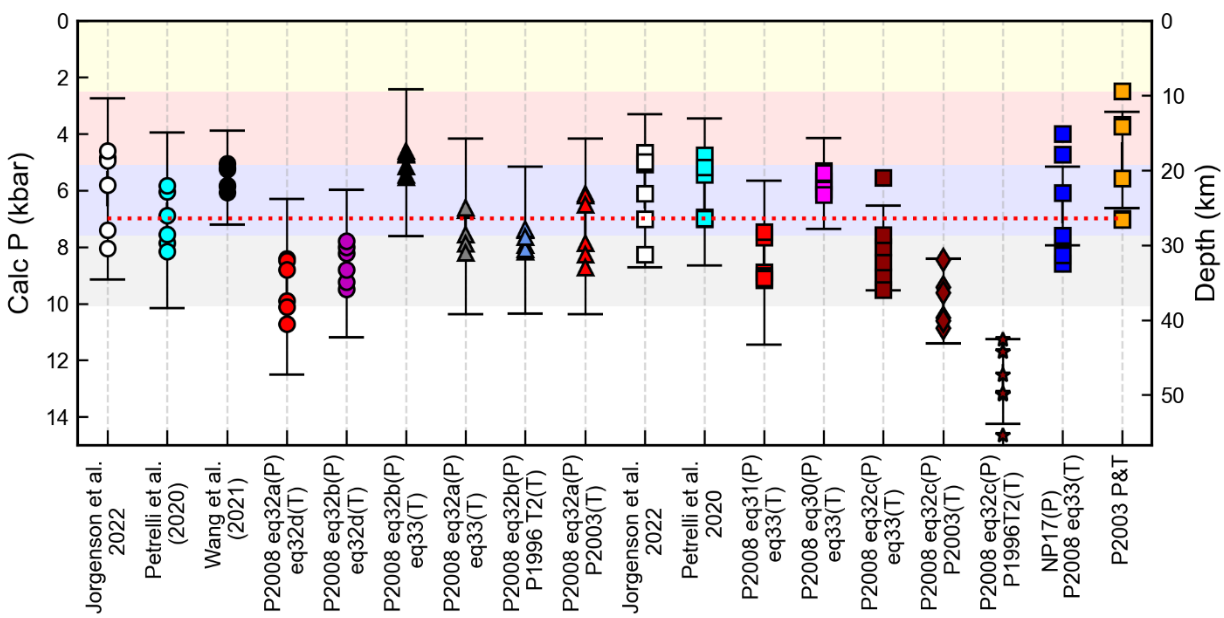

Supporting Fig. 1 – Comparison of different barometers as in Fig. 1a in the main text, but for 7 kbar experiments from Blatter et al. (2013)

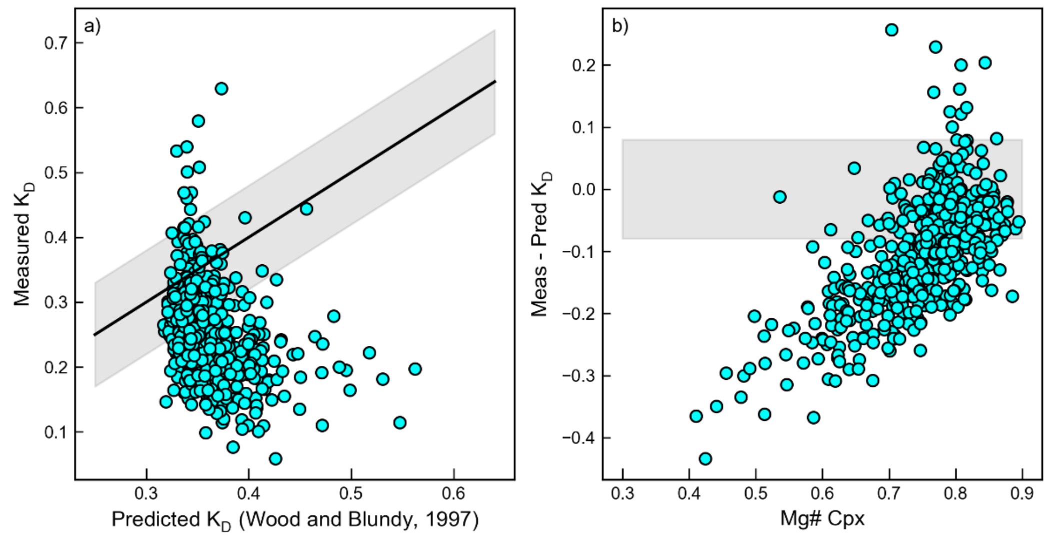

Supporting Fig. 2. Comparison of predicted and measured K_D using Wood and Blundy (1997). There is a clear offset between the measured and predicted K_D value, and the Mg# of the Cpx, with the equation performing very poorly for low Mg# Cpx.

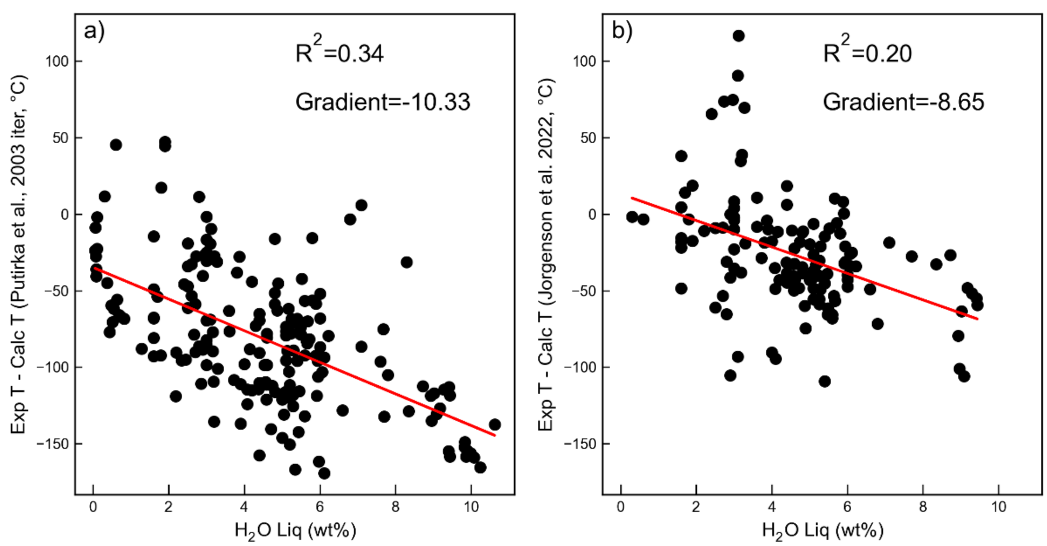

Supporting Fig. 3 – a) The discrepancy between calculated and experimental temperature iterating the thermometer and barometer of Putirka et al. (2003) increases with increasing H_2O content in the liquid. This is not surprising, given this equation has no term for H_2O, but is concerning given this equation is still used for arc magmas (see Table 1 in the main text). b) The Cpx-Liq thermometer of Jorgenson et al. (2022) also doesn't contain a H_2O term. However, the discrepancy between experimental and calculated temperature shows a much less strong correlation with water content (lower R^2, less negative gradient).

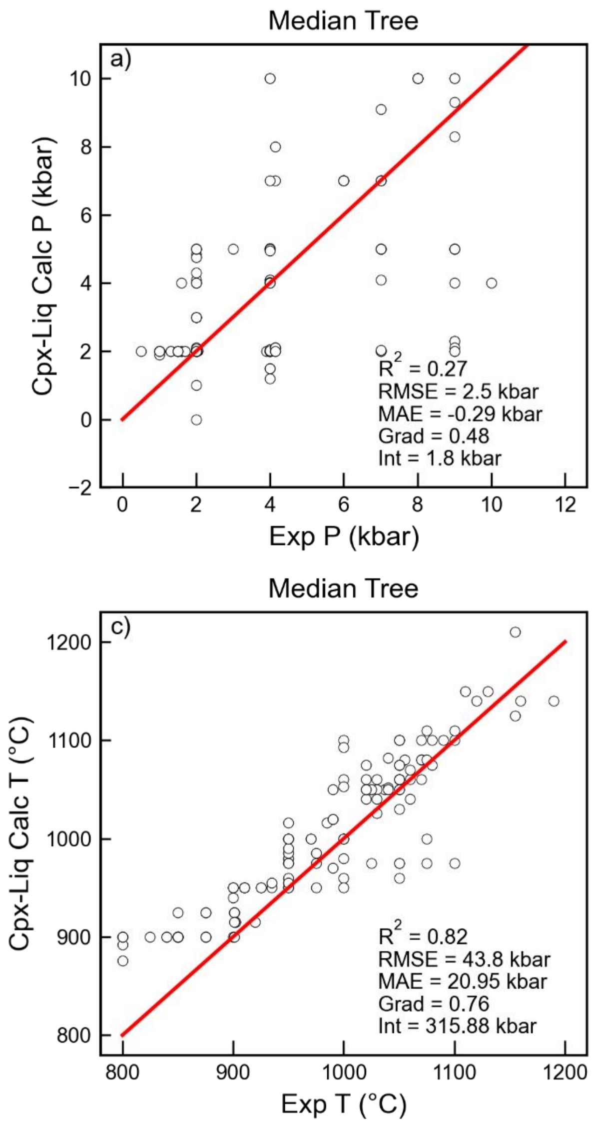

Supporting Fig 4 – Comparison of statistics using Median and mean tree for Cpx-Liq thermobarometry for Jorgenson et al. (2022).

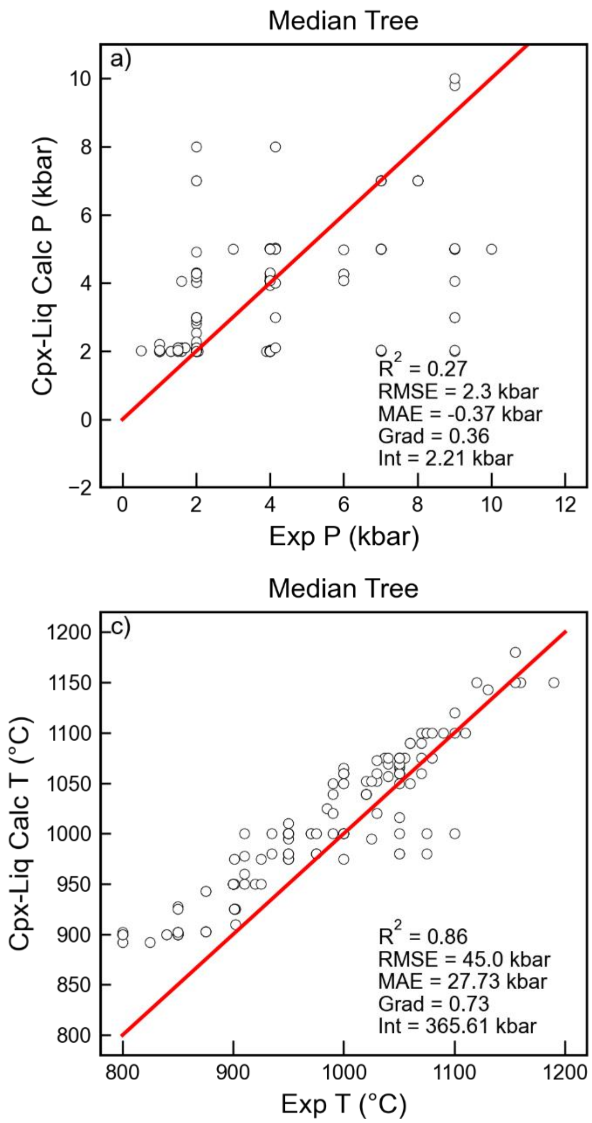

Supporting Fig. 5– Comparison of statistics using Median and mean tree for Cpx-Liq thermobarometry for Petrelli et al. (2020).

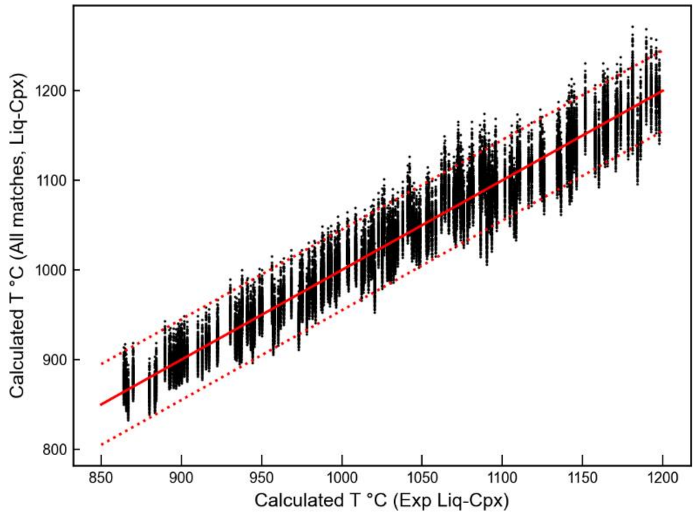

Supporting Fig 6 – Assessing the influence of the Cpx composition on the Cpx-Liq temperature. For each experimental Cpx-Liq pair we calculate the temperature using equation 33 of Putirka (2008), and plot this on the x axis. We then consider all possible Cpx-Liq matches, so each liquid gets matched to all N=194 Cpx compositions. We calculate the temperature for each of these pairs, resulting in N=194 dots sitting above each x axis coordinate. The y scatter is relatively small, the offset in calculated temperature for changing the Cpx composition is comparable to the quoted RMSE on the thermometer (shown by red dashed lines about the 1:1 red solid line). We use the average experimental pressure of the entire experimental database for all calculations.

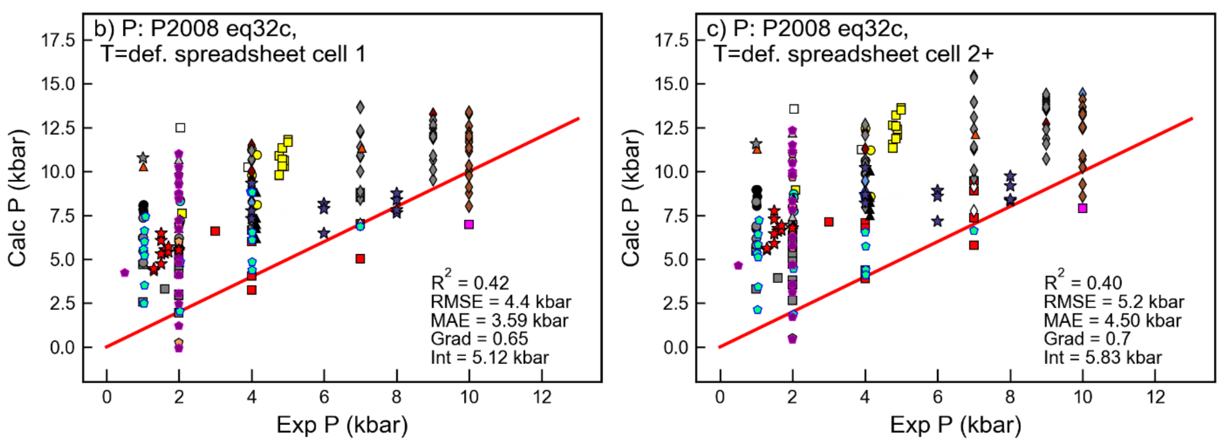

Supporting Fig. 7 – Comparing calculated and experimental pressures for the two ways Eq32c is used in the P2008 spreadsheets (the first cell vs later cells). We do not know for any given study how they dragged the cells down.

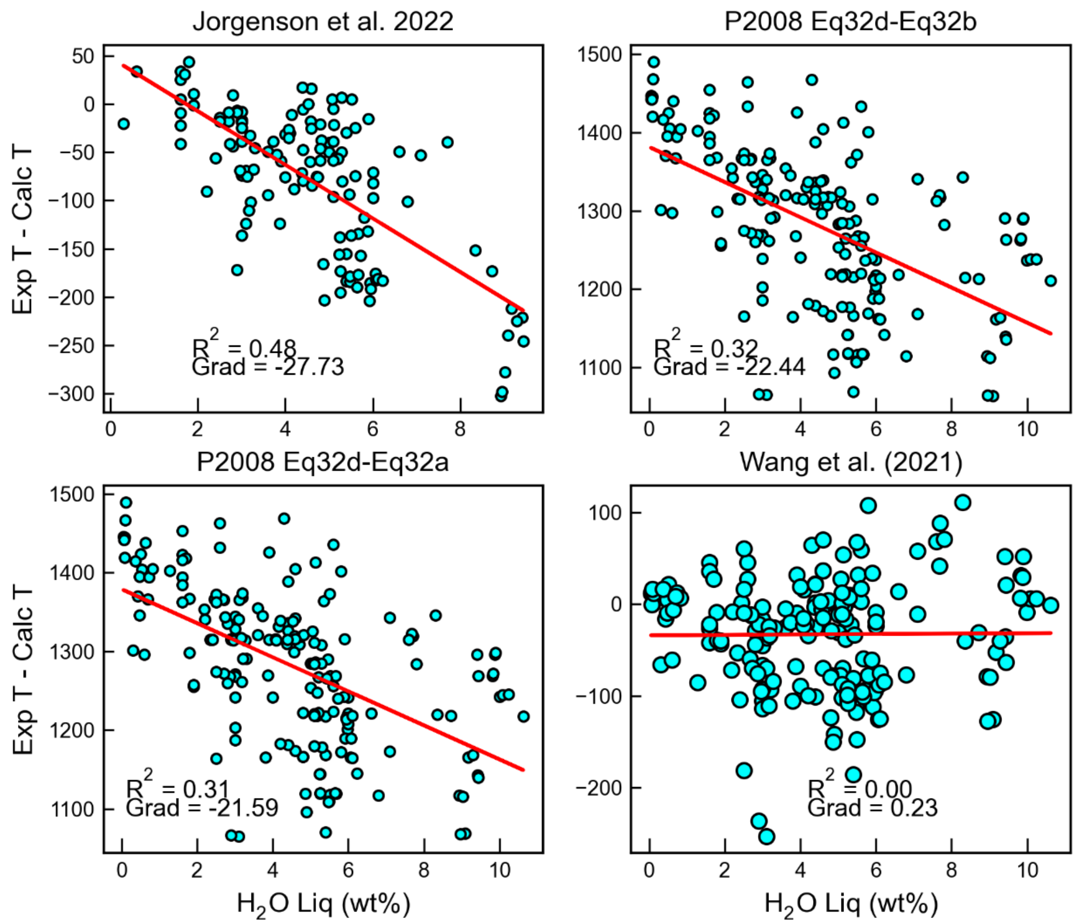

Supporting Fig 8 – Discrepancy between Cpx-only temperatures and melt water contents. Only the thermometer of Wang et al. (2021) has a term for H_2O content in the liquid.

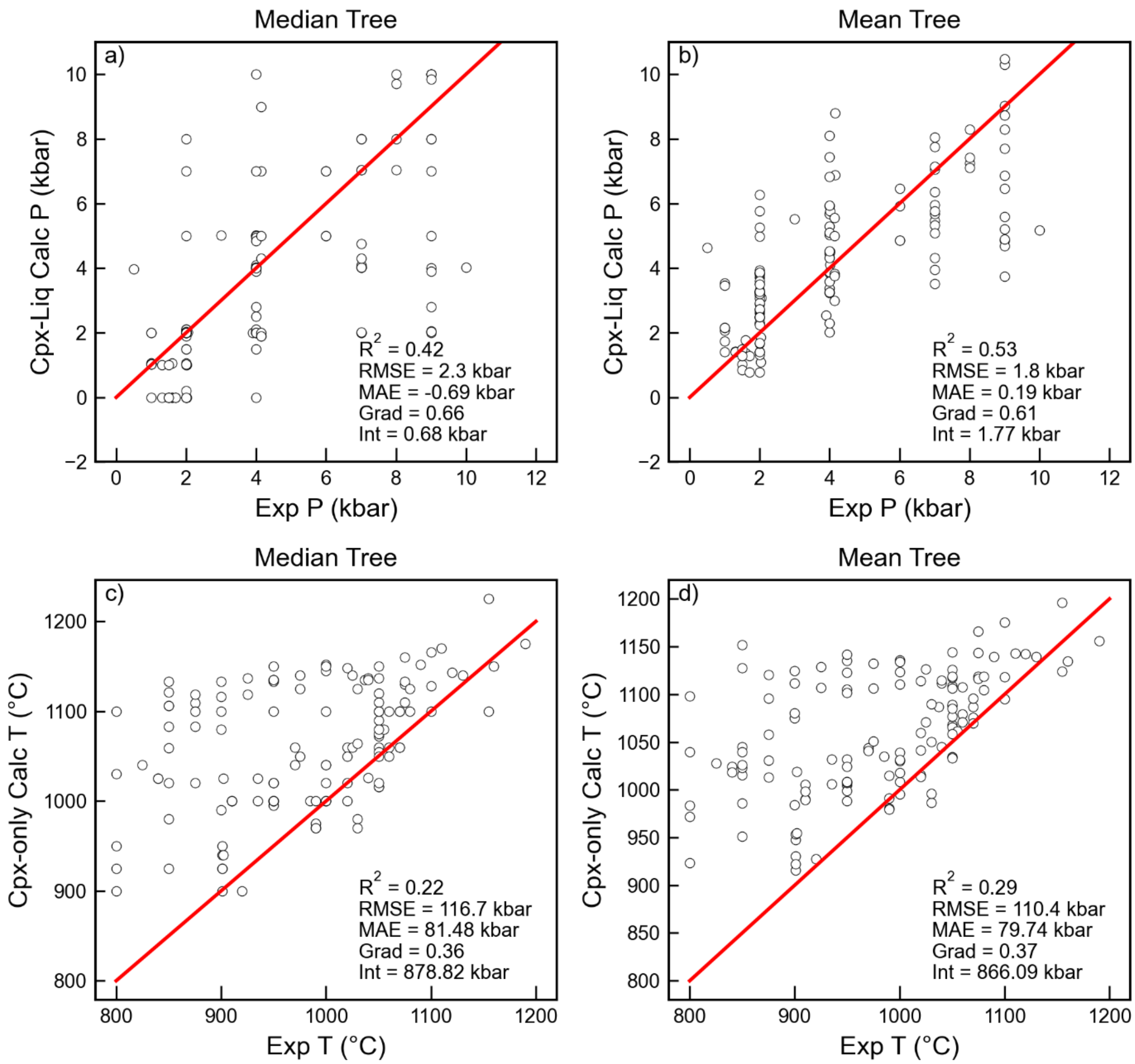

Supporting Fig 9 – Comparison of statistics using Median and mean tree for Cpx-only thermobarometry for Jorgenson et al. (2022).

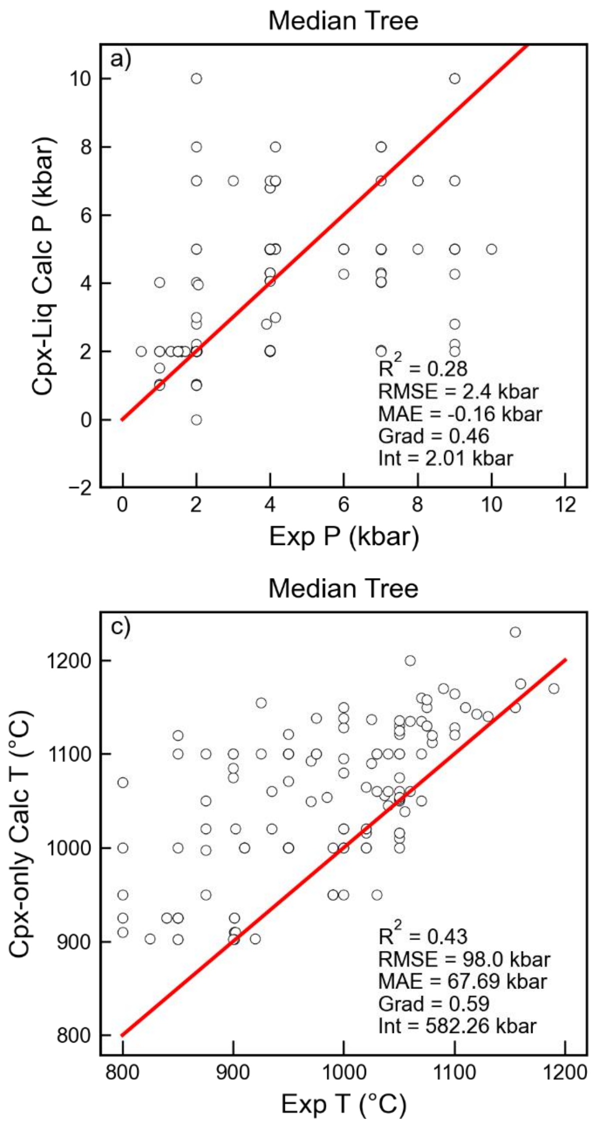

Supporting Fig. 10 – Comparison of statistics using Median and mean tree for Cpx-Liq thermobarometry for Petrelli et al. (2020).

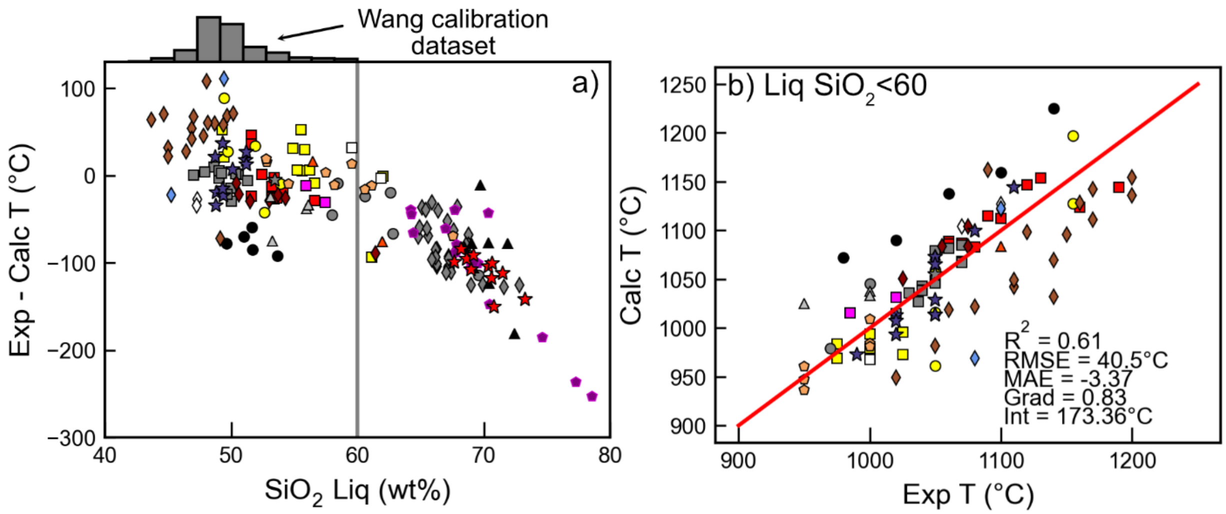

Supporting Fig 11 – Discrepancy between experimental and calculated Cpx-only temperatures using Wang et al. (2021) correlates strongly with SiO_2 when applied to Cpx grown from liquids which are more evolved than the calibration range of the model (shown by the grey histogram). Using only experiments with <60 wt% SiO2 results in a far better statistics than shown in the main text.

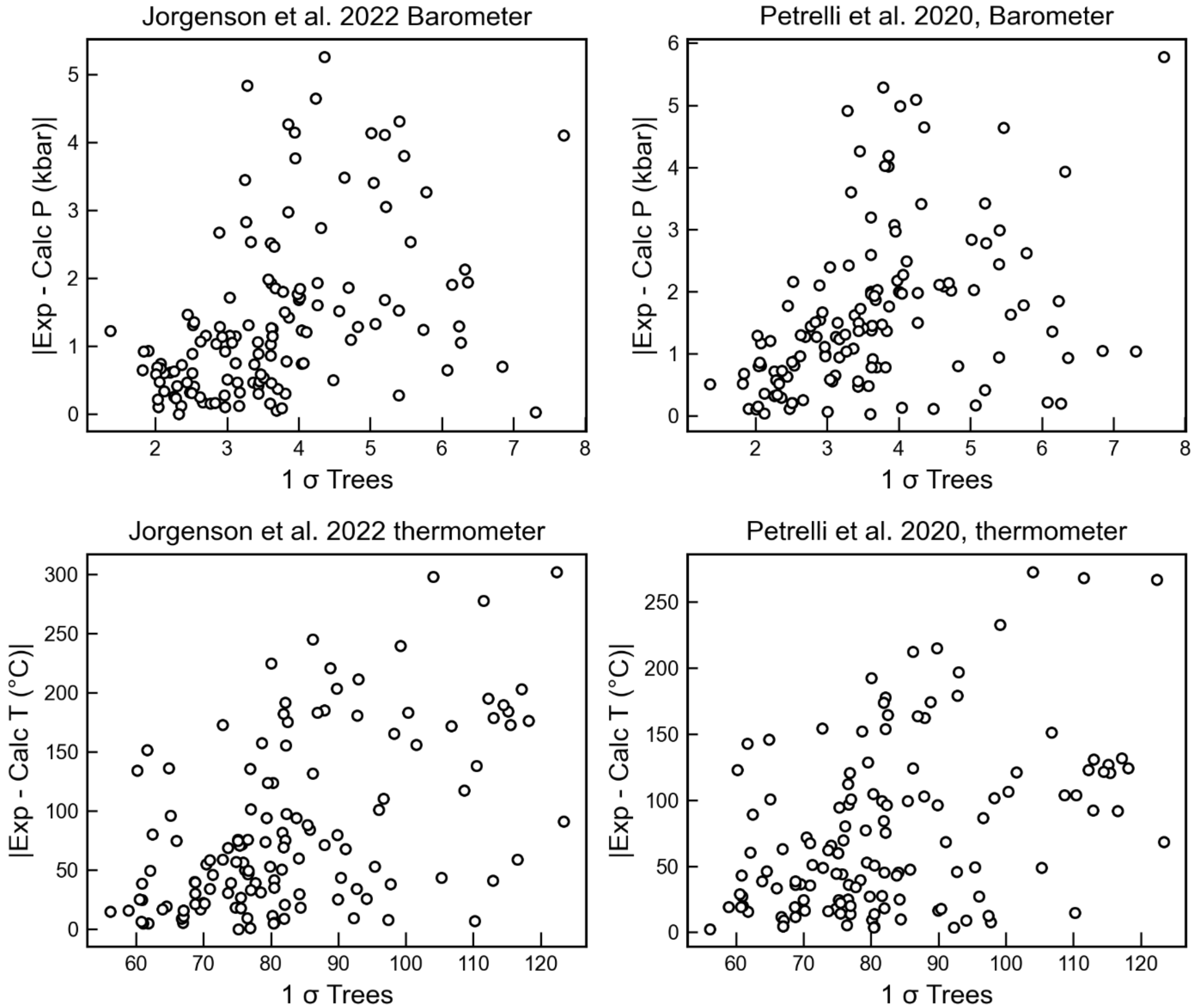

Supporting Fig. 12 – Discrepancy of calculated P and T vs. the 1 sigma value for each regression tree, which Jorgenson suggested could be a useful proxy to remove poor results.

a) Wang et al. (2021) Cpx-only

Multiple Comparison of Means - Tukey HSD, FWER=0.05

group1	group2	meandiff	p-adj	lower	upper	reject
0-2.51 kbar	2.51-5.1 kbar	2.486	0.0	1.6124	3.3597	True
0-2.51 kbar	5.1-7.6 kbar	2.7823	0.0	1.7087	3.8559	True
0-2.51 kbar	7.6-10.1 kbar	3.7507	-0.0	2.6991	4.8022	True
2.51-5.1 kbar	5.1-7.6 kbar	0.2963	0.9139	-0.8829	1.4755	False
2.51-5.1 kbar	7.6-10.1 kbar	1.2646	0.0267	0.1054	2.4238	True
5.1-7.6 kbar	7.6-10.1 kbar	0.9683	0.2269	-0.3481	2.2848	False

b) Jorgenson et al. (2022) Cpx-only

Multiple Comparison of Means - Tukey HSD, FWER=0.05

group1	group2	meandiff	p-adj	lower	upper	reject
0-2.51 kbar	2.51-5.1 kbar	2.161	0.0	1.3369	2.985	True
0-2.51 kbar	5.1-7.6 kbar	3.1183	0.0	2.1038	4.1329	True
0-2.51 kbar	7.6-10.1 kbar	4.3207	-0.0	3.3271	5.3143	True
2.51-5.1 kbar	5.1-7.6 kbar	0.9573	0.1212	-0.1611	2.0758	False
2.51-5.1 kbar	7.6-10.1 kbar	2.1597	0.0	1.0603	3.2592	True
5.1-7.6 kbar	7.6-10.1 kbar	1.2024	0.0636	-0.0463	2.451	False

c) P2008 Eq33 - NP17 Cpx-Liq

Multiple Comparison of Means - Tukey HSD, FWER=0.05

group1	group2	meandiff	p-adj	lower	upper	reject
0-2.51 kbar	2.51-5.1 kbar	3.0184	0.0	1.6104	4.4264	True
0-2.51 kbar	5.1-7.6 kbar	3.3923	0.0	1.6806	5.104	True
0-2.51 kbar	7.6-10.1 kbar	3.8679	0.0	2.1898	5.5459	True
2.51-5.1 kbar	5.1-7.6 kbar	0.3739	0.9517	-1.4656	2.2133	False
2.51-5.1 kbar	7.6-10.1 kbar	0.8495	0.6126	-0.9588	2.6577	False
5.1-7.6 kbar	7.6-10.1 kbar	0.4756	0.9307	-1.578	2.5291	False

d) Jorgenson et al. (2022) Cpx-Liq

Multiple Comparison of Means - Tukey HSD, FWER=0.05

group1	group2	meandiff	p-adj	lower	upper	reject
0-2.51 kbar	2.51-5.1 kbar	0.9497	0.0114	0.1607	1.7388	True
0-2.51 kbar	5.1-7.6 kbar	2.3443	0.0	1.3728	3.3157	True
0-2.51 kbar	7.6-10.1 kbar	3.3	-0.0	2.3486	4.2514	True
2.51-5.1 kbar	5.1-7.6 kbar	1.3945	0.0051	0.3236	2.4655	True
2.51-5.1 kbar	7.6-10.1 kbar	2.3503	0.0	1.2975	3.403	True
5.1-7.6 kbar	7.6-10.1 kbar	0.9557	0.1649	-0.2399	2.1513	False

Supporting Fig. 13– Tukey pair-wise test statistics for the bin averages shown in Fig. 15 of the main text. Comparisons highlighted red have means which are not statistically significant at p=0.05.